On the typical and atypical solutions to the Kuramoto equations*

Tianran Chen†, Evgeniia Korchevskaia‡, and Julia Lindberg§

Abstract. The Kuramoto model is a dynamical system that models the interaction of coupled oscillators. There has been much work to effectively bound the number of equilibria to the Kuramoto model for a given network. By formulating the Kuramoto equations as a system of algebraic equations, we first relate the complex root count of the Kuramoto equations to the combinatorics of the underlying network by showing that the complex root count is generically equal to the normalized volume of the corresponding adjacency polytope of the network. We then give explicit algebraic conditions under which this bound is strict and show that there are networks where the Kuramoto equations have infinitely many equilibria.

Key words. Kuramoto model, adjacency polytope, Bernshtein-Kushnirenko-Khovanskii bound

AMS subject classifications. 14Q99, 65H10, 52B20

1. Introduction.

The Kuramoto model [24] is a mathematical model that describes the dynamics on networks of oscillators. It has applications in neuroscience, biology, chemistry and power systems [4, 16, 19, 34]. Despite its simplicity, it exhibits interesting emergent behaviors. Of interest is the phenomenon of frequency synchronization which is when the oscillators synchronize to a common frequency. Frequency synchronizations correspond to solutions of the *Kuramoto equations*

$$\overline{w} = w_i - \sum_{j=0}^{n} k_{ij} \sin(\theta_i - \theta_j) \quad \text{for } i = 0, \ldots, n,$$

in the unknowns $\theta_0, \ldots, \theta_n$. Here, $\overline{w}, w_0, \ldots, w_n, k_{ij}$ are network parameters. This paper aims to understand the structure of these solutions in "typical" and "atypical" networks.

Earlier work focused on the statistical analysis of infinite networks [24] but more recently, tools from differential and algebraic geometry have enabled analysis of synchronizations on finite networks. For a finite network, knowing the total number of synchronization configurations is fundamental to understanding this model. From a computational perspective, this knowledge also plays a critical role in developing numerical methods for finding synchronization configurations. For instance, this number serves as a stopping criterion for *monodromy* algorithms [28] and allows for the development of specialized *homotopy* algorithms [7, 9] for finding all synchronization configurations.

In 1982, Ballieul and Byrnes introduced root counting techniques from algebraic geometry to this field and showed that a Kuramoto network of N oscillators has at most $\binom{2N-2}{N-1}$ synchronization configurations [2]. It coincides with the bound on the root count for the closely related load-flow equations discovered by Li, Sauer, and Yorke [26]. Algebraic geometers will recognize this bound as the bi-homogeneous Bézout bound for an algebraic version of the Kuramoto equations. This upper bound can be reached when the network is complete and complex roots are counted. However, for sparse networks, the root count (even counting complex roots) can be significantly lower than this upper bound [18, 31], demonstrating the need for a network-dependent root count.

Guo and Salam initiated one of the first algebraic analyses on such sparsity-dependent root counts [18]. Molzahn, Mehta, and Niemerg provided computational evidence for the connection

*Submitted to the editors DATE.

Funding: TC and EK are supported by a grant from the Auburn University at Montgomery Research Grant-in-Aid Program and the National Science Foundation under Grant No. 1923099. TC and JL are supported by the National Science Foundation under Grant No. 2318837. EK is also supported by the Undergraduate Research Experience program funded by the Department of Mathematics at Auburn University at Montgomery.

†Department of Mathematics, Auburn University at Montgomery, Montgomery, AL (ti@nranchen.org)

‡School of Mathematics, Georgia Institute of Technology

§Department of Mathematics, University of Texas at Austin, Austin, TX (julia.lindberg@math.utexas.edu)

between this root count and network topology [31]. In the special case of rank-one coupling coefficients, Coss, Hauenstein, Hong and Molzahn proved this complex root count to be $2^N - 2$, which is also an asymptotically sharp bound on the real root count [14]. Chen, Davis and Mehta gave a sharp bound on the complex root count for cycle networks of $N\binom{N-1}{\lfloor (N-1)/2 \rfloor}$ [11], which is asymptotically smaller than the bi-homogeneous Bézout bound discovered by Baillieul and Byrnes, proving that sparse networks have significantly fewer synchronization configurations. Interestingly, Lindberg, Zachariah, Boston, and Lesieutre showed that this bound is attainable by real roots [29]. This bound is an instance of the "adjacency polytope bound" [8], which motivates the following.

Question 1.1. *For generic choices of network parameters, does the complex root count for the algebraic Kuramoto equations reach the adjacency polytope bound for all networks?*

In the first part of this paper, we provide a positive answer to this question and thus establish the generic root count for the Kuramoto equations derived from a graph G to be the normalized volume of the adjacency polytope of G. As a corollary, we show that the Kuramoto equations are Bernshtein-general. We note that this result is similar to recent work in [5] which shows that the number of (approximate) complex solutions to the Duffing equations is generically the volume of the *Oscillator polytope*. We also extend this generic root count result to variations of the Kuramoto equations, including a special case of the power flow equations from electric engineering.

While the complex root count for the algebraic Kuramoto equations is generically constant and finite, there may be network parameters that produce different root counts. First, we focus on the role played by the coupling coefficients in such exceptional situations.

Question 1.2. *What are conditions on the coupling coefficients under which the algebraic Kuramoto equations are* not *Bernshtein-general?*

In the second part of this paper, we provide an explicit, combinatorial description for such exceptional coupling coefficients. In particular, we show that the set of exceptional coupling coefficients can be characterized by "balanced subnetworks".

For the Kuramoto equations with exceptional coupling coefficients, there are two possibilities. Either all complex solutions remain isolated but the total number drops below the generic root count, or non-isolated solution components appear. In the second case, there are infinitely many solutions, forming curves, surfaces, or geometric structures of even higher dimension.

Ashwin, Bick, and Burylko analyzed non-isolated solutions in complete networks of identical oscillators [1]. A concrete example of a network of four identical oscillators with uniform coupling coefficients was described in [14, Example 2.1]. Non-isolated solutions for cycle networks was discovered by Lindberg, Zachariah, Boston and Lesieutre [29]. Recent work by Sclosa shows that for every $d \geq 1$ there is a Kuramoto network whose stable equilibria form a manifold of dimension d [35], which, arguably, shows that the study of non-isolated solutions deserves more serious attention. This is further supported by the recent paper of Harrington, Schenck, and Stillman [20], which shows that for any 2-connected graph that contains a 3-let, there are parameters for which the Kuramoto equations have a non-isolated solution set. It is within this context, that the third part of this paper aims to provide some explicit and constructive answers to the following.

Question 1.3. *What are the conditions on the network parameters under which the Kuramoto equations have infinitely many solutions?*

The rest of this paper is structured as follows. Section 2 reviews concepts and notation that will be used. We then consider the generic root count of the Kuramoto equations in Section 3 and provide a positive answer to Question 1.1. Next, we turn our attention to non-generic coupling coefficients in Section 4 and answer Question 1.2 with a combinatorial description of the exceptional coupling coefficients. Using this description, in Section 5 we answer Question 1.3 by identifying network parameters where the Kuramoto equations have non-isolated solutions and we construct explicit parameterizations for these solutions. Finally, we conclude with a few remarks in Section 6.

2. Notation and preliminaries.

Column vectors, representing points of a lattice $L \cong \mathbb{Z}^n$, are denoted by lowercase letters with an arrowhead, e.g., $\vec{a}$. We use boldface letters, e.g., $\boldsymbol{x}$, for points in $\mathbb{C}^n$, $\mathbb{R}^n$, or $L^\vee \cong \mathbb{Z}^n$, and they are written as row vectors. For $\boldsymbol{x} = (x_1, \dots, x_n)$ and $\vec{a} = (a_1, \dots, a_n)^\top \in \mathbb{Z}^n$, $\boldsymbol{x}^{\vec{a}} = x_1^{a_1} \cdots x_n^{a_n}$ is a *Laurent monomial* with the convention that $x_i^0 = 1$, for any x_i. A linear combination of such monomials $f = \sum_{\vec{a} \in S} \boldsymbol{x}^{\vec{a}}$ is called a *Laurent polynomial*, and its *support* and *Newton polytope* are denoted $\operatorname{supp}(f) = S$ and $\operatorname{Newt}(f) = \operatorname{conv}(S)$, respectively. With respect to a vector $\boldsymbol{v}$, the *initial form* of f is $\operatorname{init}_{\boldsymbol{v}}(f)(\boldsymbol{x}) := \sum_{\vec{a} \in (S)_{\boldsymbol{v}}} c_{\vec{a}}\, \boldsymbol{x}^{\vec{a}}$, where $(S)_{\boldsymbol{v}}$ is the subset of S on which the linear functional $\langle\, \boldsymbol{v} \,,\, \bullet \,\rangle$ is minimized. For an integer matrix $A = [\vec{a}_1 \ \cdots \ \vec{a}_m]$, $\boldsymbol{x}^A := (\boldsymbol{x}^{\vec{a}_1}, \dots, \boldsymbol{x}^{\vec{a}_m})$ defines a function on the *algebraic torus* $(\mathbb{C}^*)^n = (\mathbb{C} \setminus \{0\})^n$ whose group structure is given by $(x_1, \dots, x_n) \circ (y_1, \dots, y_n) := (x_1 y_1, \dots, x_n y_n)$. We fix G to be a connected graph with vertex set $\mathcal{V}(G) = \{0, 1, \dots, n\}$ and edge set $\mathcal{E}(G)$. For nodes i and j in $\mathcal{V}(G)$, $i \sim j$ indicates their adjacency. Arrowheads will be used to distinguish digraphs from graphs, e.g., $\vec{G}$ represents a digraph and G an undirected graph. Appendix A has the full list of notation.

2.1. The Kuramoto model.

A network of coupled oscillators can be naively thought of as a swarm of points on the complex plane pulling on one another with varying force while circling around the origin. It can be used to model a wide variety of seemingly unrelated phenomena ranging from the firing of neurons and the rhythmic contractions of heart cells, to the oscillations of concentrations of chemical compounds in a mixture. In this paper, such a network is represented by a connected graph G whose nodes and edges represent the oscillators and their connections, respectively. Each oscillator has a natural frequency w_i and along the edges in G, nonzero constants $K = \{k_{ij}\}$ with $k_{ij} = k_{ji}$ quantify the coupling strength between oscillators i and j. The data structure $(G, K, \vec{w})$ encoding this model will simply be called a **network**. The Kuramoto model describes the nonlinear interactions among the oscillators by the differential equations

$$\frac{d\theta_i}{dt} = w_i - \sum_{j \sim i} k_{ij} \sin(\theta_i - \theta_j) \quad \text{for } i = 0, \dots, n, \tag{2.1}$$

where θ_i is the phase angle of the i-th oscillator [24]. *Frequency synchronization configurations* are defined to be values of $(\theta_0, \dots, \theta_n)$ at which $\frac{d\theta_i}{dt}$ equals $\overline{w} = \frac{1}{n} \sum_{i=0}^n w_i$. By adopting a rotational frame, we can assume $\theta_0 = 0$. Since $k_{ij} = k_{ji}$, we can also eliminate one equation. Therefore, frequency synchronization configurations are zeroes to the system of n transcendental functions:

$$(w_i - \overline{w}) - \sum_{j \sim i} k_{ij} \sin(\theta_i - \theta_j) \quad \text{for } i = 1, \dots, n. \tag{2.2}$$

The problem of counting synchronization configurations is therefore a root counting problem.

2.2. Algebraic Kuramoto equations.

To leverage the power of algebraic geometry, the above transcendental system can be reformulated into an algebraic system via the change of variables $x_i = e^{\mathrm{i}\theta_i}$. Then $\sin(\theta_i - \theta_j) = \frac{1}{2\mathrm{i}}(\frac{x_i}{x_j} - \frac{x_j}{x_i})$, and (2.2) becomes

$$f_{G,i}(x_1, \dots, x_n) = \overline{w}_i - \sum_{j \sim i} a_{ij} \left(\frac{x_i}{x_j} - \frac{x_j}{x_i} \right) \quad \text{for } i = 1, \dots, n, \tag{2.3}$$

where $a_{ji} = a_{ij} = \frac{k_{ij}}{2\mathrm{i}}$, $\overline{w}_i = w_i - \overline{w}$, and $x_0 = 1$. The Laurent polynomial system $\vec{f}_G = (f_{G,1}, \dots, f_{G,n})^\top$ will be called the **algebraic Kuramoto system**, and it captures all synchronization configurations in the sense that the real zeros to (2.2) correspond to the complex zeros of (2.3) on the real torus $(S^1)^n$ (i.e., $|x_i| = |e^{\mathrm{i}\theta}| = 1$). Note that f_G depends on $K = \{k_{ij}\}$ and $\vec{w}$, and we will use the notation $f_{(G,K)}$ or $f_{(G,K,\vec{w})}$ when these dependencies are emphasized.

In much of this paper, we relax the root-counting problem by considering all $\mathbb{C}^*$-zeros of (2.3). One important observation is that we can focus on graphs with no pendant (a.k.a. leaf) nodes.

Lemma 2.1. *[27, Theorem 2.5.1] Suppose $v \neq 0$ is a pendant node of G. Let $G' = G - \{v\}$. Then any $\mathbb{C}^*$-zero of $\vec{f}_{G'}$ extends to two distinct $\mathbb{C}^*$-zeros for $\vec{f}_G$.*

2.3. Kuramoto equations with phase delays. In models with phase delays, we may introduce parameters $\{\delta_{ij} \in \mathbb{R} \mid i \sim j\}$, so that along an edge $\{i,j\}$, oscillator i responds not directly to the phase angle of oscillator j but its delayed phase $\theta_j - \delta_{ij}$ [36]. Then (2.2) is generalized into:

$$0 = w_i - \overline{w} - \sum_{j \sim i} k_{ij} \sin(\theta_i - \theta_j + \delta_{ij}), \quad \text{for } i = 1, \dots, n.$$

Letting $C_{ij} = e^{\mathbf{i}\delta_{ij}}$, we can again make this system algebraic giving:

$$f_{G,i}(x_1, \dots, x_n) = \overline{w}_i - \sum_{j \sim i} a_{ij} \left(\frac{x_i C_{ij}}{x_j} - \frac{x_j}{x_i C_{ij}} \right), \quad \text{for } i = 1, \dots, n. \tag{2.4}$$

This system differs from (2.3) in the coefficients. Yet, the same set of monomials are involved, and as we will demonstrate, the algebraic arguments we will develop can be applied to this generalization.

2.4. Power flow equations. The *PV power flow system* is one important variation of the Kuramoto system. In it, the graph G models an electric power network where $\mathcal{V}(G) = \{0, \dots, n\}$ represent buses in the power network. An edge $\{i,j\} \in \mathcal{E}(G)$, representing the connection between buses i and j, has a known complex admittance $g'_{ij} + \mathrm{i} b'_{ij}$. For each bus i, the relationship between its complex power injection $P_i + \mathrm{i} Q_i$ and the complex voltages is captured by the nonlinear equations

$$P_i = \sum_{j \sim i} |V_i||V_j| (g'_{ij} \cos(\theta_i - \theta_j) + b'_{ij} \sin(\theta_i - \theta_j)) \tag{2.5}$$

$$Q_i = \sum_{j \sim i} |V_i||V_j| (g'_{ij} \sin(\theta_i - \theta_j) - b'_{ij} \cos(\theta_i - \theta_j)) \tag{2.6}$$

where $|V_i|$ is the voltage magnitude at bus i and θ_i is its phase angle. We fix bus 0 to be the *slack bus* with $\theta_0 = 0$. For a complete treatment of the derivation of the power flow equations see [17].

A node i is a *PV node* when Q_i and θ_i are unknown while P_i and $|V_i|$ are known and it models a generator bus. As above, with $x_i = e^{\mathrm{i}\theta_i}$ we get the **PV algebraic power flow equations**

$$f_{G,i}(x_1, \dots, x_n) = P_i - \sum_{j \sim i} g_{ij} \left(\frac{x_i}{x_j} + \frac{x_j}{x_i} \right) + b_{ij} \left(\frac{x_i}{x_j} - \frac{x_j}{x_i} \right), \quad \text{for } i = 1, \dots, n \tag{2.7}$$

where $b_{ij} = \frac{1}{2\mathrm{i}} |V_i||V_j| b'_{ij}$ and $g_{ij} = \frac{1}{2} |V_i||V_j| g'_{ij}$. When $g_{ij} = 0$, the corresponding power system is *lossless* and (2.7) reduces to (2.3). Otherwise, the system is *lossy* and (2.7) differs from (2.3). This is, again, a variation of the algebraic Kuramoto system (2.3) that involves the same monomials.

2.5. BKK bound. The root counting arguments in this paper revolve around the Bernshtein-Kushnirenko-Khovanskii (BKK) bound, especially Bernshtein's Second Theorem.

Theorem 2.2 (D. Bernshtein 1975 [3]). *(A) For a square Laurent system $\vec{f} = (f_1, \dots, f_n)$, if for all nonzero vectors $\vec{v} \in \mathbb{R}^n$, $\mathrm{init}_{\vec{v}}(\vec{f})$ has no $\mathbb{C}^*$-zeros, then all $\mathbb{C}^*$-zeros of $\vec{f}$ are isolated, and the total number, counting multiplicity, is the mixed volume $M = \mathrm{MV}(\mathrm{Newt}(f_1), \dots, \mathrm{Newt}(f_n))$.*

(B) If $\mathrm{init}_{\vec{v}}(\vec{f})$ has a $\mathbb{C}^*$-zero for some $\vec{v} \neq \vec{0}$, then the number of isolated $\mathbb{C}^*$-zeros $\vec{f}$ has, counting multiplicity, is strictly less than M if $M > 0$.

A system for which condition (A) holds is said to be *Bernshtein-general*. Only the special case of identical Newton polytopes, i.e., when $\mathrm{Newt}(f_1), \dots, \mathrm{Newt}(f_n)$ are all identical, will be used. This specialized version strengthens Kushnirenko's Theorem [25].

2.6. Randomized algebraic Kuramoto system. The analysis of the algebraic Kuramoto system (2.3) can be further simplified through "randomization". For any nonsingular square matrix R, the systems $\vec{f}_G$ and $\vec{f}^*_G := R \vec{f}_G$ have the same zero set. With a generic choice of R, there will be no complete cancellation of terms, and $\vec{f}_G^*$ will be referred to as the **randomized (algebraic) Kuramoto system**. This system is *unmixed* in the sense that $f_{G,1}^*, \dots, f_{G,n}^*$ have identical supports since they involve the same set of monomials, namely, constant terms and $\{x_i x_j^{-1}, x_j x_i^{-1}\}_{\{i,j\} \in \mathcal{E}(G)}$.

The randomization $\vec{f}_G \mapsto \vec{f}_G^*$ does not alter the zero set but makes a very helpful change to the tropical structure: There is a mapping between the graph-theoretical features of G and the tropical structures of $\vec{f}_G^*$ through which we can gain key insight into the structure of the zeros of $\vec{f}_G^*$.

2.7. Adjacency polytopes. For each $i = 1, \dots, n$, $\operatorname{supp}(f_{G,i}^*)$ are all identical and given by

$$\check{\nabla}_G := \{\pm(\vec{e}_i - \vec{e}_j) \mid i \sim j\} \,\cup\, \{\vec{0}\},$$

where $\vec{e}_i$ is the i-th standard basis vector of $\mathbb{R}^n$ for $i = 1, \dots, n$, and $\vec{e}_0 = \vec{0}$. The $\operatorname{conv}(\check{\nabla}_G)$ is the *adjacency polytope* or *symmetric edge polytope* of G [8, 11, 13, 30], and is related to *root polytopes* [33]. It has appeared in number theory and discrete geometry (see the overview provided in [15]).

We will not distinguish $\check{\nabla}_G$ from $\operatorname{conv}(\check{\nabla}_G)$, e.g., a "face" of $\check{\nabla}_G$ refers to a subset $F \subseteq \check{\nabla}_G$ such that $\operatorname{conv}(F)$ is a face of $\operatorname{conv}(\check{\nabla}_G)$. The facets and boundary of $\check{\nabla}_G$ are denoted $\mathcal{F}(\check{\nabla}_G)$ and $\partial\check{\nabla}_G$, respectively. $\check{\nabla}_G$ is centrally symmetric, and both $\check{\nabla}_G$ and $\partial\check{\nabla}_G$ have unimodular triangulations.

By Kushnirenko's Theorem [25], $\operatorname{Vol}(\check{\nabla}_G)$ is an upper bound for the $\mathbb{C}^*$-root count for $\vec{f}_G^*$ and $\vec{f}_G$ and the real root count to (2.2). This is the *adjacency polytope bound* [8, 11].

2.8. Faces and face subgraphs. There is an intimate connection between faces of $\check{\nabla}_G$ and subgraphs of G. Since $\vec{0}$ is an interior point of $\check{\nabla}_G$, every vertex of a proper face F of $\check{\nabla}_G$ is of the form $\vec{e}_i - \vec{e}_j$ for some $\{i,j\} \in \mathcal{E}(G)$. Thus, it is natural to consider the corresponding *facial subgraph* G_F and *facial subdigraph* $\vec{G}_F$ involving a subsets of nodes and edges sets

$$\begin{aligned} \mathcal{E}(G_F) &= \{\{i,j\} \mid \vec{e}_i - \vec{e}_j \in F \text{ or } \vec{e}_j - \vec{e}_i \in F\} \text{ and} \\ \mathcal{E}(\vec{G}_F) &= \{(i,j) \mid \vec{e}_i - \vec{e}_j \in F\}. \end{aligned}$$

As defined in [7, 15], for $F \in \mathcal{F}(\check{\nabla}_G)$, G_F is called a *facet subgraph* and $\vec{G}_F$ is a *facet subdigraph*. Higashitani, Jochemko, and Michałek provided a topological classification of face subgraphs [22, Theorem 3.1] and it was later reinterpreted [10, Theorem 3]. We state the latter here.

Theorem 2.3 (Theorem 3 [10]). *Let H be a nontrivial connected subgraph of G.*
1. *H is a face subgraph of G if and only if it is a maximal bipartite subgraph of $G[\mathcal{V}(H)]$.*
2. *H is a facet subgraph of G if and only if it is a maximal bipartite subgraph of G.*

Here, $G[V]$ is the subgraph induced by the subset $V \subset \mathcal{V}(G)$. Multiple faces can correspond to the same facial subgraph. The crisper parameterization is given by the correspondence $F \mapsto \vec{G}_F$. Reference [10] describes a necessary balancing conditions for facial subdigraphs.

For a facial subdigraph $\vec{G}_F$, its *reduced incidence matrix* $\check{Q}(\vec{G}_F)$ is the matrix with columns $\vec{e}_i - \vec{e}_j$ for $(i,j) \in \mathcal{E}(\vec{G}_F)$. Its null space can be interpreted as the space of circulations of $\vec{G}_F$.

For a subdigraph $\vec{H}$ of $\vec{G}$, the *coupling vector* $\boldsymbol{k}(\vec{H})$ has entries k_{ij} for $(i,j) \in \vec{H}$. Similarly, the entries of $\boldsymbol{a}(\vec{H})$ are the complexified coupling coefficients $a_{ij} = \frac{k_{ij}}{2\mathrm{i}}$. The ordering of the entries is arbitrary, but when appearing in the same context with $\check{Q}(\vec{H})$, consistent ordering is implied.

2.9. Facial systems. The vast literature on the facial structure of $\check{\nabla}_G$ gives us a shortcut to understanding the initial systems of $\vec{f}_G^*$, since they have particularly simple descriptions corresponding to proper faces of $\check{\nabla}_G$. For any $0 \neq \boldsymbol{v} \in \mathbb{R}^n$, the initial system $\operatorname{init}_{\boldsymbol{v}}(\vec{f}_G^*)$ is

$$\operatorname{init}_{\boldsymbol{v}}(f_{G,i}^*)(\boldsymbol{x}) = \sum_{\vec{e}_j - \vec{e}_{j'} \in F} c_{i,j,j'}\, \boldsymbol{x}^{\vec{e}_j - \vec{e}_{j'}} = \sum_{(j,j') \in \mathcal{E}(\vec{G}_F)} c_{i,j,j'}\, \boldsymbol{x}^{\vec{e}_j - \vec{e}_{j'}} \quad \text{for } i = 1, \dots, n, \tag{2.8}$$

where F is the face of $\check{\nabla}_G$ for which $\boldsymbol{v}$ is an inner normal vector. We will make frequent use of this geometric interpretation and therefore it is convenient to slightly abuse the notation and write $\operatorname{init}_F(\vec{f}_G^*) := \operatorname{init}_{\boldsymbol{v}}(\vec{f}_G^*)$. It will be called a *facial system* of $\vec{f}_G^*$, (or a *facet system* if $F \in \mathcal{F}(\check{\nabla}_G)$).

3. Generic $\mathbb{C}^*$-root count.

In this section, we establish the $\mathbb{C}^*$-root count for the algebraic Kuramoto system (2.3) for generic choices of real or complex parameters $\{\overline{w}_i\}_{i\in\mathcal{V}(G)}$ and $\{k_{ij}\}_{\{i,j\}\in\mathcal{E}(G)}$. Since $\mathbb{R}$ is Zariski-dense in $\mathbb{C}$, it is sufficient to consider generic choices of complex parameters. We show that the generic $\mathbb{C}^*$-root count is the adjacency polytope bound $\operatorname{Vol}(\check{\nabla}_G)$. A corollary is that this system is Bernshtein-general, despite the constraints on the coefficients.

There are three main obstacles. First, in each polynomial the monomials x_i/x_j and x_j/x_i share the same coefficient a_{ij}. Second, for any edge $\{i,j\}\in\mathcal{E}(G)$, the i-th and j-th polynomials have the terms $a_{ij}(x_i x_j^{-1} - x_j x_i^{-1})$ and $a_{ji}(x_j x_i^{-1} - x_i x_j^{-1})$, respectively, which are negations of each other since $a_{ij} = a_{ji}$. Therefore, the allowed choices of coefficients consists of a nowhere dense subset of (Lebesgue) measure 0 in the space of all possible complex coefficients. Finally, unless G is the complete graph, the Newton polytopes of the algebraic Kuramoto system are not full-dimensional which prevents simpler arguments (e.g. [6]) from being applied. We will show that despite these, the maximum $\mathbb{C}^*$-root count, given by the adjacency polytope bound is generically attained.

Before presenting the main theorem of this section, we first establish a few technical results that will be used, some of which are well known but are nonetheless included for completeness.

Lemma 3.1. *The lifting function $\tilde{\omega} : \check{\nabla}_G \to \mathbb{Q}$, given by*

$$\tilde{\omega}(\vec{a}) = \begin{cases} 0 & \text{if } \vec{a} = \vec{0} \\ 1 & \text{otherwise} \end{cases}$$

induces a regular subdivision $\Sigma_{\tilde{\omega}}(\check{\nabla}_G) = \{\vec{0} \cup F \mid F \in \mathcal{F}(\check{\nabla}_G)\}$.

This is a well known consequence of assigning a sufficiently small lifting value to an interior point of a point configuration ($\vec{0}$ in this case). The resulting regular subdivision may be too coarse to be useful in our discussions. Indeed, it will not be a triangulation unless G is has no even cycles [9, 10]. It can be refined into a triangulation through perturbations on the nonzero lifting values.

Lemma 3.2. *For generic but symmetric choices $\{\delta_{ij} = \delta_{ji} \in \mathbb{R} \mid \{i,j\} \in \mathcal{E}(G)\}$ that are sufficiently close to 0, the function $\omega : \check{\nabla}_G \to \mathbb{Q}$, given by*

$$\omega(\vec{a}) = \begin{cases} 0 & \text{if } \vec{a} = \vec{0} \\ 1 + \delta_{ij} & \text{if } \vec{a} = \vec{e}_i - \vec{e}_j \end{cases}$$

induces a regular unimodular triangulation $\Delta_\omega = \Sigma_\omega(\check{\nabla}_G)$ that is a refinement of $\Sigma_{\tilde{\omega}}(\check{\nabla}_G)$ and its cells are in one-to-one correspondence with cells in a unimodular triangulation of $\partial\check{\nabla}_G$. Indeed, each cell is of the form $0 \cup \Delta$ where Δ is a simplex in $\partial\check{\nabla}_G$.

Proof. We first show the interior point $\vec{0}$ is contained in every cell. Fix a $C \in \Delta_\omega$ and let $(\boldsymbol{v}, 1)$ be an inner normal vector of the lower facet of $\check{\nabla}_G^\omega$ whose projection is C. Suppose $\vec{0} \notin C$, then C contains an affinely independent set of $n+1$ points $\{\vec{a}_0, \dots, \vec{a}_n\} \not\ni \vec{0}$, and $\vec{v}$ satisfies the equation

$$\begin{bmatrix} \vec{a}_1^\top - \vec{a}_0^\top \\ \vdots \\ \vec{a}_n^\top - \vec{a}_0^\top \end{bmatrix} \boldsymbol{v}^\top = \begin{bmatrix} \omega(\vec{a}_0) - \omega(\vec{a}_1) \\ \vdots \\ \omega(\vec{a}_0) - \omega(\vec{a}_n) \end{bmatrix}.$$

Let B be the matrix on the left and $\vec{\beta}$ be the vector on the right, then $\boldsymbol{v}^\top = B^{-1}\vec{\beta}$ and thus

$$|\langle \boldsymbol{v}, \vec{a} \rangle| \le \|\boldsymbol{v}^\top\| \|\vec{a}\| \le \|\vec{a}\| \, \|B^{-1}\| \, \|\vec{\beta}\| \quad \text{for any } \vec{a} \in C.$$

Note that entries of $\vec{\beta}$ are differences among the $\{\delta_{ij}\}$. Therefore, for any $\epsilon > 0$, there is a δ such that $|\delta_{ij}| < \delta$ for all $\{i,j\} \in \mathcal{E}(G)$ implies $|\langle \boldsymbol{v}, \vec{a} \rangle| < \epsilon$, contradicting with the assumption that

$$\langle \boldsymbol{v}, \vec{a} \rangle + \omega(\vec{a}) < \langle \boldsymbol{v}, \vec{0} \rangle + \omega(\vec{0}) = 0.$$

This shows that $\vec{0}$ must be contained in every cell.

To show Δ_ω is a triangulation, it is sufficient to show nonzero points in a cell $C \in \Delta_\omega$ are assigned independent lifting values by ω. If both $\pm(\vec{e}_i - \vec{e}_j) \in C$, for some $\{i, j\} \in \mathcal{E}(G)$, then

$$\langle \boldsymbol{v} , \pm(\vec{e}_i - \vec{e}_j) \rangle + \omega(\pm(\vec{e}_i - \vec{e}_j)) = h,$$

where $h = \min\{\langle \boldsymbol{v} , \vec{a} \rangle + \omega(\vec{a}) \mid \vec{a} \in \check{\nabla}_G\}$. Since $\omega(\pm(\vec{e}_i - \vec{e}_j)) = 1 + \delta_{ij}$, summing the two produces

$$h = 1 + \delta_{ij} > 0,$$

which contradicts the constraint that $0 = \langle \vec{v}, \vec{0} \rangle + \omega(\vec{0}) \geq h$ for δ_{ij}'s sufficiently close to 0. Therefore, if $\vec{e}_i - \vec{e}_j \in C$, then $\vec{e}_j - \vec{e}_i \notin C$. Consequently, the nonzero points in C are associated with independent and generic choices of lifting values, and thus C must be a simplex.

For unimodularity, note that, since $\vec{e}_i - \vec{e}_j \in C$ implies $\vec{e}_j - \vec{e}_i \notin C$ for $\{i, j\} \in \mathcal{E}(G)$ and for a cell $C \in \Delta_\omega$, the nonzero points of C, as vectors, are exactly columns of (signed) incidence matrix of G, which is unimodular. Therefore, each cell of Δ_ω is unimodular.

Finally, to show that Δ_ω is a refinement of $\Sigma_{\tilde{\omega}}(\check{\nabla})$ from Lemma 3.1, we fix an arbitrary ordering of the points in $\check{\nabla}_G$ and consider lifting functions ω and $\tilde{\omega}$, as vectors in $\mathbb{R}^{|\check{\nabla}_G|}$. Let $\mathcal{C} = \mathcal{C}(\check{\nabla}_G, \Delta_\omega)$ be the (closed) secondary cone of Δ_ω in $\check{\nabla}_G$. Then $\mathcal{C}$ is full-dimensional, since Δ_ω is a triangulation. By assumption, ω is sufficiently close to $\tilde{\omega}$, so $\tilde{\omega} \in \mathcal{C}$, and $\Delta_\omega = \Sigma_\omega(\check{\nabla}_G)$ equals or refines $\Sigma_{\tilde{\omega}}(\check{\nabla}_G)$. ■

A lifting function $\omega : \check{\nabla}_G \to \mathbb{Q}$ for which Lemma 3.2 holds will be called a **generic symmetric lifting function** for $\check{\nabla}_G$. We now turn our attention to its graph-theoretic consequences.

Lemma 3.3. *For a generic symmetric lifting function ω for $\check{\nabla}_G$, let Δ be a simplex in Δ_ω. Then the digraph $\vec{G}_\Delta$ is acyclic, and its underlying graph G_Δ is a spanning tree of G.*

The proof of this lemma is nearly identical to the proof of [7, Theorem 1] and we include an elementary proof in Appendix B for completeness. Finally, we show a facet system derived from a spanning tree has exactly one $\mathbb{C}^*$-root, and it is nonsingular.

Lemma 3.4. *Suppose $\vec{T} < \vec{G}$ is a acyclic, and its underlying graph T is a spanning tree of G, then, for generic $\overline{w}_1, \ldots, \overline{w}_n \in \mathbb{C}^*$ and any choices of $a_{ij} \in \mathbb{C}^*$, the system of n Laurent polynomials*

$$\overline{w}_i - \sum_{j : i \rightsquigarrow j} a_{ij} \frac{x_i}{x_j} + \sum_{j : j \rightsquigarrow i} a_{ij} \frac{x_j}{x_i} \quad \textit{for } i = 1, \ldots, n$$

has a unique zero in $(\mathbb{C}^*)^n$, and this zero is isolated and regular. Here, $j \rightsquigarrow i$ means $(j, i) \in \mathcal{E}(\vec{T})$.

Proof. We prove this by induction on the number of vertices of G, N. Denote the above system as $\vec{f}_{\vec{T}}(x_0, \ldots, x_{N-1})$. The statement is true for the case where $N = 2$ and $|\mathcal{V}(G)| = |\mathcal{V}(T)| = 2$.

Assume the statement is true for any graph with N nodes and consider the case G has $N + 1$ nodes. By re-labeling, we can assume node N is a leaf in T and is adjacent to node $N - 1$. Since this system is homogeneous of degree 0, we can deviate from our convention that $x_0 = 1$ and scale the homogeneous coordinates so that $x_{N-1} = 1$. Then the above system is decomposed as the Laurent system $\vec{f}_{\vec{T}'}(x_0, \ldots, x_{N-1})$ and the binomial $\overline{w}_N \pm a_{N,N-1} x_N^{\mp 1}$, where $\vec{T}' = \vec{T} - \{N\}$. The induction hypothesis, that $\vec{f}_{\vec{T}'}(x_0, \ldots, x_N)$ has a unique isolated and regular thus completes the proof. ■

With these technical preparations, we now establish the main theorem of this section.

Theorem 3.5. *For generic choices of real or complex constants $\overline{w}_1, \ldots, \overline{w}_n$ and generic but symmetric choices of real or complex coupling coefficients $\{k_{ij} = k_{ji} \neq 0 \mid \{i, j\} \in \mathcal{E}(G)\}$, the $\mathbb{C}^*$-zeros of the algebraic Kuramoto system (2.3) are isolated and nonsingular, and the total number is* $\operatorname{Vol}(\check{\nabla}_G)$.

This is a far generalization of [11, Corollary 9 and Theorem 16] and [18, Theorem 3.3.3] where the generic $\mathbb{C}^*$-root count is established for tree[1], cycle, and complete networks only.

[1]The generic number of complex equilibria for the Kuramoto model on tree networks is 2^n. This fact appears to be well known among researchers in power systems long before the referenced paper [11].

Proof. By Sard's Theorem, for generic choices of $\overline{w}_1, \ldots, \overline{w}_n$, the $\mathbb{C}^*$-zero set of $\vec{f}_G$ consists of isolated and regular points. Under this assumption, we only need to establish the $\mathbb{C}^*$-root count. Moreover, since it is already known this root count is bounded by $\mathrm{Vol}(\check{\nabla}_G)$, it is sufficient to show that it is greater than or equal to this bound. We shall take a constructive approach through a specialized version of the polyhedral homotopy of Huber and Sturmfels [23].

Let $\omega : \check{\nabla}_G \to \mathbb{Q}$ be a generic symmetric lifting function for $\check{\nabla}_G$. We use the notation $\omega_{ij} = \omega(\vec{e}_i - \vec{e}_j) = \omega(\vec{e}_j - \vec{e}_i)$ and define the function $\vec{h} = (h_1, \ldots, h_n) : (\mathbb{C}^*)^n \times \mathbb{C} \to \mathbb{C}^n$, given by

$$h_i(x_1, \ldots, x_n, t) = \overline{w}_i - \sum_{j \sim i} a_{ij} t^{\omega_{ij}} \left(\frac{x_i}{x_j} - \frac{x_j}{x_i} \right).$$

Away from $t = 0$, $\vec{h}$ is a parameterized version of the original system $\vec{f}_G$ with coefficients being analytic functions of the parameter t. Note that since $\omega_{ij} = \omega_{ji}$, for any choice of $t \in \mathbb{C}$, the system still satisfies the symmetry constraints on the coefficients. By the Parameter Homotopy Theorem [32], for t outside a proper Zariski closed (i.e., finite) set $Q \subset \mathbb{C}$, the number of isolated $\mathbb{C}^*$-zeros of $\vec{h}(\,\cdot\,, t) = 0$ is a constant which is also an upper bound for the isolated $\mathbb{C}^*$-root count for $\vec{h}(\,\cdot\,, t)$ for all $t \in \mathbb{C}$. Let η be this generic $\mathbb{C}^*$-root count. Since $\overline{w}_i$ and a_{ij} are chosen generically, and $\vec{h}(\,\cdot\,, 1) \equiv \vec{f}_G(\,\cdot\,)$, we can conclude that $t = 1$ is outside Q and thus η agrees with the generic $\mathbb{C}^*$-root count of $\vec{f}_G$ that we aims to establish. That is, it is sufficient to show $\eta \geq \mathrm{Vol}(\check{\nabla}_G)$.

Taking a constructive approach, we now construct η smooth curves (of one real-dimension), that will connect the $\mathbb{C}^*$-zeros of $\vec{f}_G$ and the collection of $\mathbb{C}^*$-zeros of the special systems described in Lemma 3.4. This connection allows us to count the number of curves.

Along a ray $t : (0, 1] \to \mathbb{C}$ on the complex plane parameterized by $t(\tau) = \tau e^{i\theta}$ for a choice of $\theta \in [0, 2\pi)$ that avoids Q (i.e., $t(\tau) \notin Q$ for all $\tau \in (0, 1]$), the function $\vec{h}$ is given by

$$h_i(x_1, \ldots, x_n, t) = h_i(x_1, \ldots, x_n, \tau e^{i\theta}) = \overline{w}_i - \sum_{j \sim i} a_{ij} e^{i\theta\omega_{ij}} \tau^{\omega_{ij}} \left(\frac{x_i}{x_j} - \frac{x_j}{x_i} \right),$$

and $\vec{h}$ has η isolated and regular $\mathbb{C}^*$-zeros for all $\tau \in (0, 1]$. By the principle of homotopy continuation, the zero set of $\vec{h}$ form η smooth curves in $(\mathbb{C}^*)^n \times (0, 1]$ smoothly parameterizable by τ. The problem is now reduced to counting these curves.

Fixing such a curve C, the asymptotic behavior of C as $\tau \to 0$, in a compactification of $(\mathbb{C}^*)^n$ can be characterized by the solutions to an initial system of $\vec{h}$, as a system of Laurent polynomials in $\mathbb{C}\{\tau\}[x_1^{\pm 1}, \ldots, x_n^{\pm 1}]$. Stated in affine coordinates, by the Fundamental Theorem of Tropical Geometry, there exists a system of convergent Puiseux series $x_1(\tau), \ldots, x_n(\tau) \in \mathbb{C}\{\tau\}$ that represents the germ of C, as an analytic variety, at $\tau = 0$, such that the leading coefficients, as a point in $(\mathbb{C}^*)^n$ satisfies the initial system $\mathrm{init}_{\boldsymbol{v}}(\vec{h})$,[2] and $\boldsymbol{v} = (v_1, \ldots, v_n) \in \mathbb{Q}^n$ are the orders of the Puiseux series $x_1(\tau), \ldots, x_n(\tau) \in \mathbb{C}\{\tau\}$. Therefore, it is sufficient to show that there are at least $\mathrm{Vol}(\check{\nabla}_G)$ distinct initial systems of $\vec{h}$ that will each contribute one solution path.

By Lemma 3.2, the regular subdivision $\Delta_\omega = \Sigma_\omega(\check{\nabla}_G)$ is a unimodular triangulation. Fix a simplex $\Delta \in \Delta_\omega$, and let $(\boldsymbol{v}, 1)$ be the upward pointing inner normal vector that defines Δ, then by construction, there is an affinely independent set $\{\vec{a}_1, \ldots, \vec{a}_n\} \subset \partial\check{\nabla}_G$ such that

$$\begin{aligned} \langle \boldsymbol{v}\,,\, \vec{a}_k \rangle + \omega(\vec{a}_k) &= 0 \quad \text{for } k = 1, \ldots, n, \textit{ and} \\ \langle \boldsymbol{v}\,,\, \vec{a} \rangle + \omega(\vec{a}) &> 0 \quad \text{for all } \vec{a} \in \check{\nabla}_G \setminus \{\vec{0}, \vec{a}_1, \ldots, \vec{a}_n\}. \end{aligned}$$

Therefore, the exponent vectors associated with monomials with nonzero coefficients in $\mathrm{init}_{\boldsymbol{v}}(\vec{h})$ are exactly $\{0, \vec{a}_1, \ldots, \vec{a}_n\}$. By Lemma 3.3, $\vec{T} = \vec{G}_\Delta$ is an acyclic subdigraph and its associated

[2] We do not claim $\vec{h}$ form a tropical basis, nor do we require that $\mathrm{init}_{\boldsymbol{v}}(\vec{h})$ generate the corresponding initial ideal. Yet, as we will show, an initial system of $\vec{h}$ of the special form we will describe is sufficient to uniquely determine the leading coefficients of the Puiseux series expansion of a solution path.

subgraph T is a spanning tree of G. Indeed, $\text{init}_{\boldsymbol{v}}(\vec{h})$ consists of Laurent polynomials

$$\overline{w}_i - \sum_{j \in \mathcal{N}_T^+(i)} a_{ij} \frac{x_i}{x_j} + \sum_{j \in \mathcal{N}_T^-(i)} a_{ij} \frac{x_j}{x_i} \quad \text{for } i = 1, \ldots, n.$$

By Lemma 3.4, this system has a unique $\mathbb{C}^*$-zero, which is regular. Following from the principle of homotopy continuation, it gives rise to a smooth curve defined by $\vec{h}(\boldsymbol{x}, \tau e^{i\theta}) = 0$ in $(\mathbb{C}^*)^n \times (0, 1]$.

This holds for every simplex in Δ_ω, i.e., each simplex $\Delta \in \Delta_\omega$ contributes a curve define by $\vec{h} = \vec{0}$. Moreover, these curves are distinct, so $\eta \geq |\Delta_\omega| = \text{Vol}(\check{\nabla}_G)$, which completes the proof. ■

This establishes the fact that the generic $\mathbb{C}^*$-root count for the algebraic Kuramoto system $\vec{f}_G$ is exactly the adjacency polytope bound, despite the algebraic constraints on the parameters. Note that the BKK bound for $\vec{f}_G$ is always between the generic $\mathbb{C}^*$-root count and the adjacency polytope bound. Therefore, we can indirectly derive the Bernshtein-genericity of $\vec{f}_G$.

Corollary 3.6. *For generic real or complex $\overline{w}_1, \ldots, \overline{w}_n$ and generic but symmetric real or complex $k_{ij} = k_{ji} \neq 0$ for $\{i, j\} \in \mathcal{E}(G)$, the algebraic Kuramoto system (2.3) is Bernshtein-general, and*

$$\text{MV}(\text{Newt}(f_{G,1}), \ldots, \text{Newt}(f_{G,n})) = \text{Vol}(\text{conv}(\text{Newt}(f_{G,1}) \cup \cdots \cup \text{Newt}(f_{G,n}))) = \text{Vol}(\check{\nabla}_G).$$

Remark 3.7. We remark that the proof of Theorem 3.5 utilizes many ideas from the polyhedral homotopy of Huber and Sturmfels [23]. The main differences are that we consider a lifting function that preserves the relationships among the coupling coefficients and we choose generators of the ideals at "toric infinity" with a nice tree structure instead of requiring them to be binomial.

Finally, we draw attention to the tropical nature of this proof. The first half of the proof establishes the tropical version of the generic root count result: With the assignment of the valuation $\text{val}(\overline{w}_i) = 0$ and generic but symmetric $\text{val}(a_{ij}) = \text{val}(a_{ji}) = \omega_{ij} = \omega_{ji}$, we showed that the intersection number of the tropical hypersurfaces defined by $f_{G,1}, \ldots, f_{G,n}$ is bounded below by $\text{Vol}(\check{\nabla})$ which is also the stable self-intersection number of the tropical hypersurface defined by the randomized Kuramoto system (as defined in Subsection 2.6) with the same valuation. Computing generic root counts via stable tropical intersection is the topic of a recent paper by Paul Helminck and Yue Ren [21], in which the special case for complete networks is studied as an example.

Another consequence of Theorem 3.5 is the monotonicity of the generic $\mathbb{C}^*$-root count, since the volume of the adjacency polytope is strictly increasing as new edges and nodes are added.

Corollary 3.8. *Let $(G_1, K_1, \vec{w}_1)$ and $(G_2, K_2, \vec{w}_2)$ be two connected networks such that $G_1 < G_2$. Then the generic $\mathbb{C}^*$-root count of $\vec{f}_{G_1}$ is strictly less than that of $\vec{f}_{G_2}$.*

In addition, this shows that the phase-delayed algebraic Kuramoto system is Bernshtein-general.

Corollary 3.9. *For generic choices of $\overline{w}_i, a_{ij}, C_{ij}$, the algebraic Kuramoto systems with phase delays (2.4) is Bernshtein-general, and its $\mathbb{C}^*$-root count equals to the normalized volume of ∇_G.*

Proof. As noted before, for generic choices of $\overline{w}_1, \ldots, \overline{w}_n$, all $\mathbb{C}^*$-zeros of this system are isolated and regular. Let η be the generic number of $\mathbb{C}^*$-zeros this system has. By Theorem 2.2 and Corollary 3.6, we know $\eta \leq \text{Vol}(\check{\nabla}_G)$. By the Parameter Homotopy Theorem [32], the number of $\mathbb{C}^*$-zeros of this parameterized system constant on a nonempty Zariski open set of the parameters. By setting $C_{ij} = 1$, we recover (2.3) and by Theorem 3.5 and Corollary 3.6, this system is Bernshtein-general, with $\text{Vol}(\check{\nabla}_G)$ $\mathbb{C}^*$-zeros. This shows that $\eta \geq \text{Vol}(\check{\nabla}_G)$, giving the result. ■

From the same argument, we get the generic root count for the PV power flow equations.

Corollary 3.10. *For generic choices of P_i, b_{ij}, g_{ij}, the lossy PV-type algebraic power flow system (2.7) is Bernshtein-general, and its $\mathbb{C}^*$-root count equals to the normalized volume of $\check{\nabla}_G$.*

We conclude this section by showing some known results for volumes of adjacency polytopes in Table 3.1. We observe that for cyclic, tree and wheel networks, previous results by convex geometers

Network	Volume of adjacency polytope
A tree network with N nodes [11]	2^{N-1}
A cycle network with N nodes [11]	$N\binom{N-1}{\lfloor (N-1)/2 \rfloor}$
A complete network with N nodes [2]	$\binom{2N-2}{N-1}$
A network formed by joining k cycles of lengths $2m_1, \dots, 2m_k$, consecutively along an edge [15]	$\frac{1}{2^{k-1}} \prod_{i=1}^{k} m_i \binom{2m_i}{m_i}$
A network formed by joining two odd cycles of lengths $2m_1 + 1$ and $2m_2 + 1$ along an edge [15]	$(m_1 + m_2 + 2m_1 m_2)\binom{2m_1}{m_1}\binom{2m_2}{m_2}$
A wheel graph with $N + 1$ nodes [15]	$\begin{cases} (1-\sqrt{3})^N + (1+\sqrt{3})^N & N \text{ odd} \\ (1-\sqrt{3})^N + (1+\sqrt{3})^N - 2 & N \text{ even} \end{cases}$

Table 3.1: Known results for the volume of adjacency polytopes for families of networks.

give sharp bounds for the number of complex roots to the Kuramoto equations. Conversely, power system engineers have known for decades the complex root count of the PV power flow equations for complete networks [2]. Now due to Theorem 3.5, this gives the volume of adjacency polytopes of complete networks. This demonstrates how Theorem 3.5 bridges the two worlds.

4. Explicit genericity conditions on coupling coefficients.

So far, we have established that the generic $\mathbb{C}^*$-root count of the algebraic Kuramoto system $\vec{f}_G$ is the adjacency polytope bound, $\operatorname{Vol}(\check{\nabla}_G)$. That is, for almost all choices of the parameters $\vec{w}$ (natural frequencies) and K (coupling coefficients), the $\mathbb{C}^*$-root count for $\vec{f}_G$ is equal to $\operatorname{Vol}(\check{\nabla}_G)$. This section aims to understand exactly when the $\mathbb{C}^*$-root count drops below $\operatorname{Vol}(\check{\nabla}_G)$. We focus on the effect of coupling coefficients $\{k_{ij}\}$. The effect of natural frequencies $\vec{w}$ will be explored in Section 5.

Definition 4.1 (Exceptional coupling coefficients). *Given a connected graph G with $n+1$ nodes, we define its* ***exceptional coupling coefficients****, $\mathcal{K}^\circ(G)$, to be the set of symmetric and nonzero coupling coefficients $K = \{k_{ij}\}_{i\sim j}$ such that, counting multiplicity, the number of isolated $\mathbb{C}^*$-zeros of $\vec{f}_{(G,K,\vec{w})}$ is strictly less than $\operatorname{Vol}(\check{\nabla}_G)$, for any choice of $\vec{w} \in \mathbb{C}^n$.*

In other words, $\mathcal{K}^\circ(G)$ is the set of symmetric coupling coefficients for which the algebraic Kuramoto system (2.3) is not Bernshtein-general. In the following subsections, we will develop an algebraic and graph-theoretic description for the exceptional coupling coefficients $\mathcal{K}^\circ(G)$.

We start with the analysis of a single facial system. For a face F of $\check{\nabla}_G$, we describe the coupling coefficients for which the facial system $\operatorname{init}_F(\vec{f}^*_G)$ has a $\mathbb{C}^*$-zero, signaling the genericity condition for Theorem 3.5 is broken and the number of isolated $\mathbb{C}^*$-zeros of $\vec{f}_{(G,K)}$ drops.

Definition 4.2 (Exceptional coupling coefficients for a face). *For a proper face of $\check{\nabla}_G$, we define*

$$\mathcal{K}^\circ(\vec{G}_F) = \{\boldsymbol{k}(\vec{G}_F) \in (\mathbb{C}^*)^{|F|} \mid \operatorname{init}_F(\vec{f}^*_G) = \vec{0} \text{ has a } \mathbb{C}^*\text{-solution}\}$$

to be the set of ***exceptional coupling coefficients*** *with respect to the face F (or $\vec{G}_F$).*

It is worth noting that such exceptional coupling coefficients are extremely rare. By Theorems 2.2 and 3.5, $\mathcal{K}^\circ(\vec{G}_F)$ is contained in a proper and Zariski closed subset of Lebesgue measure zero. Yet, a full description of $\mathcal{K}^\circ(\vec{G}_F)$ is possible, as we will detail in the rest of this section. We start, in Subsection 4.1, with a "circulation" formulation of a facial system, which bridges together the algebraic and graph-theoretic sides of this problem. In Subsection 4.2, we describe a parameterization of the $\mathbb{C}^*$-zero set of a facial system. We use this parameterization in Subsection 4.3 to derive an explicit description of the exceptional coupling coefficients. Finally, we conclude this section with a few examples of global descriptions of $\mathcal{K}^\circ(G)$ in Subsection 4.4.

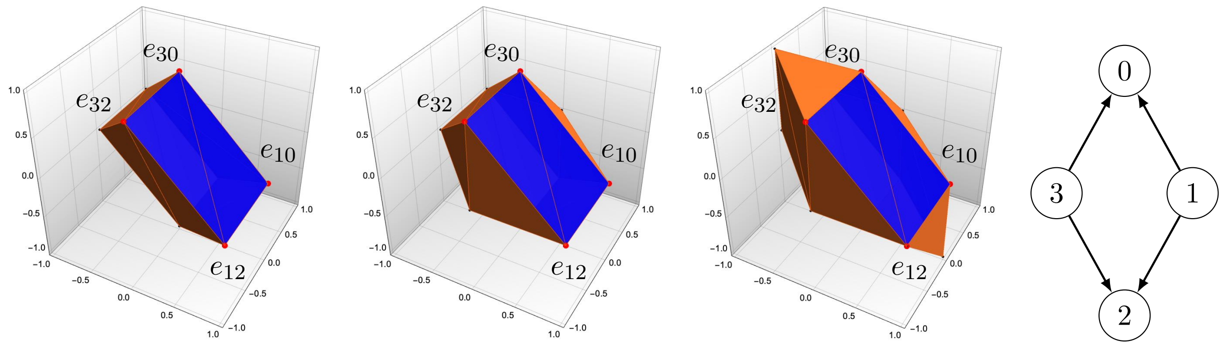

(a) AP derived from C_4 (b) AP derived from H_4 (c) AP derived from K_4 (d) Facet digraph

Figure 4.1: The adjacency polytopes of $C_4, H_4 = K_4 - \{e_{13}\}$ and K_4 with the vertex labels $e_{ij} := e_i - e_j$ together with the facet subdigraph corresponds to the common facet in blue.

4.1. Circulation forms of facial systems. To connect the abstract algebraic condition in Definition 4.1 to the concrete graph-theoretic features, we transform facial systems of $\vec{f}_G^*$ into equivalent "circulation forms", which is understood more easily from the graph-theoretical viewpoint.

Lemma 4.3. *Let $F \neq \varnothing$ be a proper face of $\check{\nabla}_G$, $\check{Q}(\vec{G}_F)$ and $\boldsymbol{a}(\vec{G}_F)$ be the corresponding reduced incidence matrix of $\vec{G}_F$ and its coupling vector, respectively. Then* $\operatorname{init}_F(\vec{f}_G^*)(\boldsymbol{x}) = \vec{0}$ *if and only if*

$$\check{Q}(\vec{G}_F)\left(\boldsymbol{x}^{\check{Q}(\vec{G}_F)} \circ \boldsymbol{a}(\vec{G}_F)\right)^\top = \vec{0}. \tag{4.1}$$

Proof. Recall that $\vec{f}_G^* = R \cdot \vec{f}_G$ for a nonsingular matrix $R = [r_{ij}]$ Since $a_{ij} = a_{ji}$, we have

$$\operatorname{init}_F(f_{G,k}^*)(\boldsymbol{x}) = \sum_{(i,j)\in\vec{G}_F} (r_{ki} - r_{kj})\, a_{ij}\, \boldsymbol{x}^{\vec{e}_i - \vec{e}_j} = \sum_{(i,j)\in\vec{G}_F} \langle\, \boldsymbol{r}_k\,,\, \vec{e}_i - \vec{e}_j\,\rangle\, a_{ij}\, \boldsymbol{x}^{\vec{e}_i - \vec{e}_j}, \quad \text{for } k = 1, \ldots, n,$$

where $\boldsymbol{r}_k$ is the k-th row of the matrix R. Since $\{\vec{e}_i - \vec{e}_j \mid (i,j) \in \mathcal{E}(\vec{G}_F)$ are the columns in $\check{Q}(\vec{G}_F)$,

$$\operatorname{init}_F(\vec{f}_G^*)(\boldsymbol{x}) = R\,\check{Q}(\vec{G}_F)\left(\boldsymbol{x}^{\check{Q}(\vec{G}_F)} \circ \boldsymbol{a}(\vec{G}_F)\right)^\top.$$

Since the square matrix R is assumed to be nonsingular, this establishes the equivalence. ■

Equation (4.1) will be referred to as the *circulation form* of the facial system $\operatorname{init}_F(\vec{f}_G^*)$ since the null space of $\check{Q}(\vec{G}_F)$ can be interpreted as the *space of circulations* of $\vec{G}_F$. Circulations on directed graphs are assignments of flows along directed edges so that the sum of incoming flows is equal to the sum of outgoing flows at each nodes. Equation (4.1) requires $\boldsymbol{x}^{\check{Q}(\vec{G}_F)} \circ \boldsymbol{a}(\vec{G}_F)$ to be a circulation on the facial digraph $\vec{G}_F$, where the flows are allowed to have complex values.

Example 4.4. Consider the facial subgraph in Figure 4.1d, which is shared by C_4, $H_4 = K_4 - \{e_{13}\}$, and K_4. The corresponding incidence and reduced incidence matrices, respectively, are

$$Q(\vec{G}_F) = \begin{array}{c} \\ 0 \\ 1 \\ 2 \\ 3 \end{array}\!\!\begin{array}{c} \begin{array}{cccc} e_{10} & e_{12} & e_{32} & e_{30} \end{array} \\ \begin{pmatrix} -1 & 0 & 0 & -1 \\ 1 & 1 & 0 & 0 \\ 0 & -1 & -1 & 0 \\ 0 & 0 & 1 & 1 \end{pmatrix} \end{array}, \qquad \check{Q}(\vec{G}_F) = \begin{array}{c} \\ 1 \\ 2 \\ 3 \end{array}\!\!\begin{array}{c} \begin{array}{cccc} e_{10} & e_{12} & e_{32} & e_{30} \end{array} \\ \begin{pmatrix} 1 & 1 & 0 & 0 \\ 0 & -1 & -1 & 0 \\ 0 & 0 & 1 & 1 \end{pmatrix} \end{array}.$$

By Lemma 4.3, the facial system $\operatorname{init}_F(\vec{f}_{C_4}^*)(\boldsymbol{x}) = \vec{0}$ is equivalent to its circulation form

$$(4.2)\quad \begin{bmatrix}0\\0\\0\end{bmatrix} = \begin{bmatrix}1 & 1 & 0 & 0\\ 0 & -1 & -1 & 0\\ 0 & 0 & 1 & 1\end{bmatrix}\left(\begin{bmatrix}x_1 & x_2 & x_3\end{bmatrix}^{\left[\begin{smallmatrix}1 & 1 & 0 & 0\\ 0 & -1 & -1 & 0\\ 0 & 0 & 1 & 1\end{smallmatrix}\right]} \circ \begin{bmatrix}a_{10} & a_{12} & a_{32} & a_{30}\end{bmatrix}\right)^\top = \begin{bmatrix}a_{10}x_1 + a_{12}\frac{x_1}{x_2}\\ -a_{12}\frac{x_1}{x_2} - a_{32}\frac{x_3}{x_2}\\ a_{32}\frac{x_3}{x_2} + a_{30}x_3\end{bmatrix}$$

Observe that adding the three equations in (4.2) together implies that at node 0 the balancing condition $-a_{10}x_1 - a_{30}x_3 = 0$ is also satisfied. Therefore, $\begin{bmatrix}a_{10}x_1 & a_{12}\frac{x_1}{x_2} & a_{32}\frac{x_3}{x_2} & a_{30}x_3\end{bmatrix}^\top$ is a nonzero circulation on $\vec{G}_F$ if and only if (4.2) is true.

This circulation form suggests a strong tie between the topological features of a facial subdigraphs $\vec{G}_F$ and the algebraic features of its facial system $\operatorname{init}_F(\vec{f}_G^*)$. The rest of this paper is devoted to exploring this connection by leveraging the wealth of existing knowledge about the facial complex of $\check{\nabla}_G$. In particular, we will show that the circulation form of facial systems produce concrete genericity conditions on the coupling coefficients. Before doing so, we state two immediate observations that simplify our discussions but defer the proofs to Appendix B.

Lemma 4.5. *For a proper face $F \neq \varnothing$ of $\check{\nabla}_G$ whose facial subdigraph $\vec{G}_F$ consists of weakly connected components $\vec{H}_1, \ldots, \vec{H}_\ell$, there exist faces $F_1, \ldots, F_\ell \neq \varnothing$ of F such that $\vec{H}_i = \vec{G}_{F_i}$ and*

$$\operatorname{init}_F(\vec{f}_G^*)(\boldsymbol{x}) = \vec{0} \quad \Longleftrightarrow \quad \operatorname{init}_{F_i}(\vec{f}_G^*)(\boldsymbol{x}) = \vec{0} \quad \text{for each } i = 1, \ldots, \ell.$$

Lemma 4.6. *For a proper face $F \neq \varnothing$ of $\check{\nabla}_G$, let $G' = G[G_F]$ and F' be the embedding of F in $\check{\nabla}_{G'}$. Then $\operatorname{init}_F(\vec{f}_G^*)$ has a $\mathbb{C}^*$-zero if and only $\operatorname{init}_{F'}(\vec{f}_{G'}^*)$ has a $\mathbb{C}^*$-zero.*

Together, these lemmas tell us that it is sufficient to focus on facial systems corresponding to facial subgraphs that are connected and spanning, which are exactly the facet systems.

4.2. Tree solutions. With our focus fixed on facet systems, we now give an explicit parameterization for the possible solution sets to a given facet system.

Definition 4.7 (Tree solutions). *For a given facet F of $\check{\nabla}_G$, let $\vec{H} = \vec{G}_F$ be its facet subdigraph. We fix a weak spanning tree $\vec{T}$, i.e., a subdigraph $\vec{T} \leq \vec{H}$ whose underlying undirected graph is a spanning tree of the underlying undirected graph of $\vec{H}$. If $\vec{T} \neq \vec{H}$, let $\vec{v}_1, \ldots, \vec{v}_d$ be the columns of $\check{Q}(\vec{H})$ corresponding to the directed edges in $\mathcal{E}(\vec{H}) \setminus \mathcal{E}(\vec{T})$, as column vectors, and let $\boldsymbol{\tau}_k = (\check{Q}(\vec{T})^{-1}\vec{v}_k)^\top$ for $k = 1, \ldots, d$. We define the **tree solution** induced by $\vec{T}$ to be*

$$(4.3)\qquad \boldsymbol{x}_{\vec{T}}(\lambda_1, \ldots, \lambda_d) = \left[\left(\sum_{k=1}^{d} \lambda_k \boldsymbol{\tau}_k\right) \circ \boldsymbol{a}_{\vec{T}}^{-I}\right]^{\check{Q}(\vec{T})^{-1}}.$$

Example 4.8 (A tree solution for C_4). Consider the graph $G = C_4$ and the subdigraph $\vec{H}$ shown in Figure 4.1d. With the choice $\vec{T} < \vec{H}$ such that $\mathcal{E}(\vec{T}) = \{(1,0), (1,2), (3,2)\}$, we have one directed edge in $\vec{H}$ that is outside $\vec{T}$, and it corresponds to the incidence vector $\vec{v}_1 = \begin{bmatrix}0 & 0 & 1\end{bmatrix}^\top$. Then

$$\boldsymbol{\tau}_1 = (\check{Q}(\vec{T})^{-1}\vec{v}_1)^\top = \left(\begin{bmatrix}1 & 1 & 0\\ 0 & -1 & -1\\ 0 & 0 & 1\end{bmatrix}^{-1} \cdot \begin{bmatrix}0\\0\\1\end{bmatrix}\right)^\top = \begin{bmatrix}1 & -1 & 1\end{bmatrix}.$$

Therefore, the tree solution induced by $\vec{T}$ is

$$\begin{aligned} x_{\vec{T}}(\lambda_1) &= \left(\lambda_1 \begin{bmatrix}1 & -1 & 1\end{bmatrix} \circ \begin{bmatrix}a_{10}^{-1} & a_{12}^{-1} & a_{32}^{-1}\end{bmatrix}\right)^{\left[\begin{smallmatrix}1 & 1 & 1\\ 0 & -1 & -1\\ 0 & 0 & 1\end{smallmatrix}\right]} \\ &= \begin{bmatrix}\lambda_1 a_{10}^{-1} & \frac{\lambda_1 a_{10}^{-1}}{-\lambda_1 a_{12}^{-1}} & \frac{\lambda_1 a_{10}^{-1}\lambda_1 a_{32}^{-1}}{-\lambda_1 a_{12}^{-1}}\end{bmatrix} \\ &= \begin{bmatrix}\frac{\lambda_1}{a_{10}} & \frac{a_{12}}{a_{10}} & \frac{-\lambda_1 a_{12}}{a_{10}a_{32}}\end{bmatrix}.\end{aligned}$$

Indeed, each tree solution provides a candidate solution in the sense that if $\operatorname{init}_F(\vec{f}_G^*)$ has a $\mathbb{C}^*$-zero, then it must be given by $\boldsymbol{x}_{\vec{T}}$ for any weak spanning tree $\vec{T}$.

Lemma 4.9. *If $\boldsymbol{x}$ is a $\mathbb{C}^*$-zero of $\operatorname{init}_F(\vec{f}_G^*)$, then for any weak spanning tree $\vec{T}$ of $\vec{G}_F$, there exists $\lambda_1, \ldots, \lambda_d \in \mathbb{C}$ such that*

$$\boldsymbol{x} = \boldsymbol{x}_{\vec{T}}(\lambda_1, \ldots, \lambda_d).$$

Proof. Let $\vec{H}$, $\vec{T}$, $\boldsymbol{\tau}_1, \ldots, \boldsymbol{\tau}_d$, $\vec{v}_1, \ldots, \vec{v}_d$, and $\boldsymbol{x}_{\vec{T}}$ be those referenced in Definition 4.7. Suppose $\boldsymbol{x}$ is a $\mathbb{C}^*$-zero of $\operatorname{init}_F(\vec{f}_G^*)$. We shall arrange the columns/entries, so that

$$\check{Q}(\vec{H}) = \begin{bmatrix} \check{Q}(\vec{T}) & \vec{v}_1 & \cdots & \vec{v}_d \end{bmatrix} \qquad \text{and} \qquad \boldsymbol{a}(\vec{H}) = \begin{bmatrix} \boldsymbol{a}(\vec{T}) & \alpha_1 & \cdots & \alpha_d \end{bmatrix}$$

where $\alpha_1, \ldots, \alpha_d$ are the complex coupling coefficients on the directed edges corresponds to $\vec{v}_1, \ldots, \vec{v}_d$.

By Lemma 4.3, the circulation form of $\operatorname{init}_F(\vec{f}_G^*)$ is

$$\check{Q}(\vec{H}) \left(\boldsymbol{x}^{\check{Q}(\vec{H})} \circ \boldsymbol{a}(\vec{H}) \right)^\top = \begin{bmatrix} \check{Q}(\vec{T}) & \vec{v}_1 & \cdots & \vec{v}_d \end{bmatrix} \begin{bmatrix} \left(\boldsymbol{x}^{\check{Q}(\vec{T})} \circ \boldsymbol{a}(\vec{T}) \right)^\top \\ \boldsymbol{x}^{\vec{v}_1} \cdot \alpha_1 \\ \vdots \\ \boldsymbol{x}^{\vec{v}_d} \cdot \alpha_d \end{bmatrix} = \vec{0}. \tag{4.4}$$

Since the null space of $\check{Q}(\vec{H})$ is spanned by $(\boldsymbol{\tau}_1, -\boldsymbol{e}_1)^\top, \ldots, (\boldsymbol{\tau}_d, -\boldsymbol{e}_d)^\top \in \mathbb{Z}^{n+d}$. There exist $\lambda_1, \ldots, \lambda_d \in \mathbb{C}$ such that

$$\sum_{k=1}^{d} \lambda_k \boldsymbol{\tau}_k = \boldsymbol{x}^{\check{Q}(\vec{T})} \circ \boldsymbol{a}(\vec{T}). \tag{4.5}$$

The conclusion thus follow from the fact that the reduced incidence matrix $\check{Q}(\vec{T})$ is unimodular. ■

Lemma 4.9 shows that any $\mathbb{C}^*$-zero of a facet system must be given by a tree solution. Indeed, (4.4) shows that with an additional condition, the converse is also true.

Corollary 4.10. *Let F, $\vec{T}$, $\boldsymbol{x}_{\vec{T}}$, and $\boldsymbol{\tau}_1, \ldots, \boldsymbol{\tau}_d$ be as in Definition 4.7, and let $\boldsymbol{\eta}_i = [\boldsymbol{\tau}_i, -\boldsymbol{e}_i]$ and $\vec{\eta}_i = \boldsymbol{\eta}_i^\top$ for $i = 1, \ldots, d$. Then, for nonzero $\lambda_1, \ldots, \lambda_d$, the tree solution $\boldsymbol{x}_{\vec{T}}(\lambda_1, \ldots, \lambda_d)$ is a solution to the facial system $\operatorname{init}_F(\vec{f}_G^*)$ if and only if*

$$\left(\sum_{k=1}^{d} \lambda_k \boldsymbol{\eta}_k \right)^{\vec{\eta}_i} \cdot \boldsymbol{a}(\vec{H})^{-\vec{\eta}_i} = 1 \quad \textit{for each } i = 1, \ldots, d.$$

An elementary proof is included in the appendix for completeness. In the following we will provide a graph-theoretic interpretation of these algebraic conditions.

4.3. Exceptional coupling characterized by balancing conditions.

Now, we will show that the exceptional coupling coefficients with respect to a face are exactly those coefficients that satisfy "balancing" conditions on the corresponding face subdigraph.

Several distinct concepts that capture intricate balancing conditions on Kuramoto networks have been studied. Following this tradition, we will define "balanced networks". Depending on the additional information we take into consideration, it has three layers of meanings.

Definition 4.11. *We say an acyclic digraph $\vec{H}$, whose underlying graph is a cycle, is **balanced** if it contains an equal number of directed edges pointing clockwise and counterclockwise.*

This definition implies that a balanced cycle must be an even cycle. In [10], it was shown that all facial subdigraphs of C_N must be balanced. Figure 4.2 shows two subdigraphs of C_4, one balanced and one unbalanced.

In addition, if we take into consideration the weights on the directed edges, i.e. the coupling coefficients in our context, we can define a stronger notion of balanced cycle.

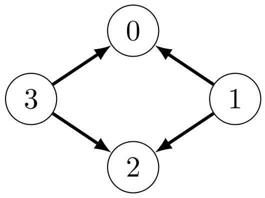

(a) Balanced: 2 counterclockwise and 2 clockwise edges

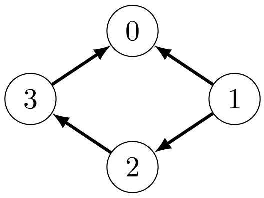

(b) Unbalanced: 1 counterclockwise and 3 clockwise edges

Figure 4.2: Balanced and unbalanced digraphs.

Definition 4.12. *We say an acyclic digraph $\vec{H}$, whose underlying graph is C_N, is **balanced with respect to the weights** $K = \{k_{ij} \mid (i,j) \in \mathcal{E}(\vec{H})\}$ if it is balanced (as in Definition 4.11) and*

$$\prod_{(i,j)\in\mathcal{E}^+(\vec{H})} k_{ij} = (-1)^{N/2} \prod_{(i,j)\in\mathcal{E}^-(\vec{H})} k_{ij}, \tag{4.6}$$

where $\mathcal{E}^+(\vec{H})$ and $\mathcal{E}^-(\vec{H})$ are the sets of edges pointing clockwise and counterclockwise, respectively.

Example 4.13. Continuing with the examples on subdigraphs of C_4, the digraph shown in Figure 4.2a is balanced with respect to $K = \{k_{ij}\}$ if and only if $k_{10}k_{32} = k_{12}k_{30}$.

It turns out that this balancing condition characterizes the exceptional coupling coefficients when the facial subgraph G_F is a cycle.

Proposition 4.14. *Let F be a face of $\check{\nabla}_G$ such that G_F is a cycle. Then the set of exceptional coupling coefficients with respect to F is*

$$\mathcal{K}^\circ(\vec{G}_F) = \{K \mid \vec{G}_F \text{ is balanced with respect to the weights assigned by } K\}.$$

Proof. By Lemma 4.6, it is sufficient to assume that G_F spans G. By Lemma 4.9, it is sufficient to consider the tree solution $\boldsymbol{x}_{\vec{T}}(\lambda)$ (Definition 4.7) induced by a weak spanning tree $\vec{T}$ of $\vec{G}_F$.

Let $\boldsymbol{\eta}^\top \in \{+1,-1\}^{n+1}$ be a primitive basis vector for $\ker \check{Q}(\vec{G}_F)$. Its entries gives the orientations of the edges in $\vec{G}_F$. Since $\vec{G}_F$ must be edge-wise balanced (Definition 4.11), exactly half of the entries in $\boldsymbol{\eta}$ is -1. By Corollary 4.10, $\boldsymbol{x}_{\vec{T}}$ parameterizes $\mathbb{C}^*$-zeros of $\operatorname{init}_F(\vec{f}_G^*)$ if and only if

$$1 = (\lambda\boldsymbol{\eta})^{\vec{\eta}} \cdot \boldsymbol{a}(\vec{G}_F)^{-\vec{\eta}} = \boldsymbol{\eta}^{\vec{\eta}} \cdot \boldsymbol{a}(\vec{G}_F)^{-\vec{\eta}} = (-1)^{N/2}\boldsymbol{a}(\vec{G}_F)^{-\vec{\eta}} = (-1)^{N/2} \prod_{(i,j)\in\mathcal{E}(\vec{G}_F)} k_{ij}^{\sigma(i,j)},$$

where $\sigma(i,j) \in \{+1,-1\}$ are the entries in $\boldsymbol{\eta}$ and they indicate the orientations of the directed edge (i,j) in $\vec{G}_F$. Rearranging factors here produces the desired equation (4.6). ∎

For subdigraphs beyond cycles, more complicated balancing conditions are required to characterize the exceptional coupling coefficients. Indeed, we need all cycles in G_F to be balanced with respect to a common circulation. Recall that a circulation on a digraph $\vec{H}$ is an assignment of weights on the edges $\eta = \{\eta_{ij} \mid (i,j) \in \mathcal{E}(\vec{H})\}$ so that the sum of the incoming and outgoing weights are balanced on each node, i.e., for each $i = 1,\dots,n$,

$$\sum_{j,(i,j)\in\mathcal{E}(\vec{H})} \eta_{ij} = \sum_{k,(k,i)\in\mathcal{E}(\vec{H})} \eta_{ki}.$$

Circulations correspond to a null vector of the reduced incidence matrix $\check{Q}(\vec{H})$. As before, we allow complex weights to be used in circulations.

Definition 4.15. *For an acyclic digraph $\vec{H}$, let H be its underlying undirected graph, let $\{C_1, \ldots, C_d\}$ be the cycles in H, and let $\vec{C}_1, \ldots, \vec{C}_d < \vec{H}$ be their corresponding digraphs.*

*We say $(\vec{H}, K)$ is **balanced with respect to a circulation** $\eta = \{\eta_{ij} \neq 0 \mid (i,j) \in \mathcal{E}(\vec{H})\}$ if $\vec{C}_1, \ldots, \vec{C}_d$ are balanced (in the sense of Definition 4.11), and*

$$\prod_{(i,j)\in\mathcal{E}^+(\vec{C}_\ell)} \frac{k_{ij}}{\eta_{ij}} = \prod_{(i,j)\in\mathcal{E}^-(\vec{C}_\ell)} \frac{k_{ij}}{\eta_{ij}}, \tag{4.7}$$

for each $\ell = 1, \ldots, d$, where $\mathcal{E}^+(\vec{C}_k)$ and $\mathcal{E}^-(\vec{C}_k)$ are the sets of directed edges of $\vec{C}_k$ in the counterclockwise and clockwise orientations, respectively.

Here, it is sufficient to restrict $\{C_1, \ldots, C_d\}$ to be a cycle basis of H. Also note that this definition takes into consideration both the weights on directed edges and a given circulation. It is a generalization of Definition 4.12 since the vector space of circulations on a cycle is 1-dimensional.

Example 4.16. Figure 4.3 shows a digraph with weighted edges. It is balanced with respect to a circulation $\eta = \{\eta_{ij}\}$ if

$$\frac{k_{50}k_{12}}{\eta_{50}\eta_{12}} = \frac{k_{10}k_{52}}{\eta_{10}\eta_{52}} \qquad \text{and} \qquad \frac{k_{52}k_{34}}{\eta_{52}\eta_{34}} = \frac{k_{54}k_{32}}{\eta_{54}\eta_{32}}. \tag{4.8}$$

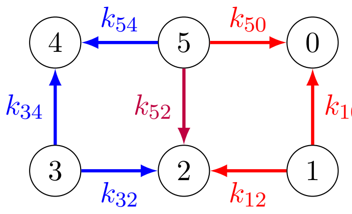

Figure 4.3: Balancing condition with respects to weights

This stronger balancing condition gives us the exact description for the exceptional coupling coefficients in the bridgeless cases. Recall, a *bridge* of a graph is an edge that is not contained in any cycle of the graph. A graph with no bridges is said to be *bridgeless*.

Theorem 4.17. *Let F be a face of $\check{\nabla}_G$.*

- *If G_F contains a bridge, then $\mathcal{K}^\circ(\vec{G}_F) = \varnothing$.*
- *If G_F is bridgeless, then*

$$\mathcal{K}^\circ(\vec{G}_F) = \{K \mid \vec{G}_F \textit{ is balanced with respect to a nonzero circulation on } \vec{G}_F\}.$$

Proof. We now consider the first case. If G_F contains a bridge, then any null vector of $\check{Q}(\vec{G}_F)$ must contain a zero entry, which corresponds to the bridge edge. By Lemma 4.9, the facial system $\operatorname{init}_F(\vec{f}^*_G)$ has no $\mathbb{C}^*$-zero for any nonzero choices of coefficients.

For the second case, as remarked earlier, we can assume G_F is both connected and spanning. Fixing any weak spanning tree $\vec{T}$ for $\vec{G}_F$, we consider the tree solution $\boldsymbol{x}_{\vec{T}}$ (Definition 4.7). Let $\boldsymbol{\tau}_1, \ldots, \boldsymbol{\tau}_d$ and $\boldsymbol{\eta}_\ell = [\boldsymbol{\tau}_\ell, -\boldsymbol{e}_\ell]$ be those referenced in Corollary 4.10.

Suppose $(\vec{G}_F, K)$ is balanced with respect to a nonzero circulation $\eta = \{\eta_{ij}\}$. Then

$$\prod_{(i,j)\in\mathcal{E}^+(\vec{C}_\ell)} \frac{k_{ij}}{\eta_{ij}} = \prod_{(i,j)\in\mathcal{E}^-(\vec{C}_\ell)} \frac{k_{ij}}{\eta_{ij}} \qquad \text{i.e.,} \qquad 1 = \prod_{(i,j)\in\mathcal{E}(\vec{C}_\ell)} \left(\frac{k_{ij}}{\eta_{ij}}\right)^{\sigma_{ij}}$$

for each $\ell = 1, \ldots, d$, where $\sigma_{ij} \in \{+1, -1\}$ indicate the orientation of the edge (i,j) in $\vec{C}_\ell$.

Recall that $\boldsymbol{\eta}_1, \ldots, \boldsymbol{\eta}_d$ spans the vector space of circulations. So after arranging $\{\eta_{ij}\}$ into a row vector $\boldsymbol{\eta}$ according to the edge ordering that is consistent with $\boldsymbol{\eta}_1, \ldots, \boldsymbol{\eta}_d$, there exist nonzero $\lambda_1, \ldots, \lambda_d$ such that $\boldsymbol{\eta} = \lambda_1\boldsymbol{\eta}_1 + \cdots \lambda_d\boldsymbol{\eta}_d$. Combining this and the previous equation, we get

$$1 = \prod_{(i,j)\in\mathcal{E}(\vec{C}_\ell)} \left(\frac{k_{ij}}{\eta_{ij}}\right)^{\sigma_{ij}} = (\lambda_1\boldsymbol{\eta}_1 + \cdots \lambda_d\boldsymbol{\eta}_d)^{\vec{\eta}_\ell}\, \boldsymbol{a}(\vec{G}_F)^{-\vec{\eta}}$$

for $\ell = 1, \ldots, d$. By Corollary 4.10, $\operatorname{init}_F(\vec{f}^*_{(G,K)})$ has a $\mathbb{C}^*$-zero, and thus the coupling coefficients given by K is among the exceptional coupling coefficients $\mathcal{K}^\circ(\vec{G}_F)$.

Conversely, if $K \in \mathcal{K}^\circ(\vec{G}_F)$, then, by Lemma 4.9, a $\mathbb{C}^*$-zeros of $\mathrm{init}_F(\vec{f}^*_{(G,K)})$ is given by the tree solution $\boldsymbol{x}_{\vec{T}}(\lambda_1,\ldots,\lambda_d)$ (Definition 4.7) for some $\lambda_1,\ldots,\lambda_d \neq 0$. Moreover, by Corollary 4.10,

$$1 = (\lambda_1 \boldsymbol{\eta}_1 + \cdots \lambda_d \boldsymbol{\eta}_d)^{\vec{\eta}_\ell}\, \boldsymbol{a}(\vec{G}_F)^{-\vec{\eta}} = \prod_{(i,j)\in\mathcal{E}(\vec{C}_\ell)} \left(\frac{k_{ij}}{\eta_{ij}}\right)^{\sigma_{ij}},$$

Since $\boldsymbol{x}_{\vec{T}}(\lambda_1,\ldots,\lambda_d) \in (\mathbb{C}^*)^n$, $\lambda_1,\ldots,\lambda_d$ are nonzero, and $\boldsymbol{\eta} = \lambda_1\boldsymbol{\eta}_1 + \cdots \lambda_d\boldsymbol{\eta}_d$ is a nonzero circulation on $\vec{G}_F$. Therefore, $(\vec{G}_F, K)$ is balanced with respect to the nonzero circulation $\boldsymbol{\eta}$. ■

Although Theorem 4.17 depends on the existence of a circulation, as Proposition 4.14 has shown, this balancing condition can be simplified in the case where G_F is a cycle. We now consider one more case in which a similar simplication can be achieved.

Proposition 4.18. *If a facial subdigraph $\vec{G}_F$ is the graph union of $\vec{C}_1,\ldots,\vec{C}_d$ whose underlying undirected graphs $C_1,\ldots,C_d$ are independent cycles of G_F sharing a single edge, then $\mathcal{K}^\circ(\vec{G}_F)$ consists of exactly the coupling coefficients for which*

$$1 = \sum_{\ell=1}^{d} (-1)^{|C_\ell|/2} \frac{\prod_{(i,j)\in\mathcal{E}^+(\vec{C}_\ell)} k_{ij}}{\prod_{(i,j)\in\mathcal{E}^-(\vec{C}_\ell)} k_{ij}}, \tag{4.9}$$

where $\mathcal{E}^+(\vec{C}_\ell)$ and $\mathcal{E}^-(\vec{C}_\ell)$ are the set of directed edges of $\vec{C}_\ell$ in the two possible orientations, respectively, and the edge shared by $C_1,\ldots,C_d$ is considered negatively oriented.

Proof. Recall that the face subgraph G_F must be bipartite (Theorem 2.3) and therefore the cycles $C_1,\ldots,C_d$ must be even.

Suppose $K = \{k_{ij}\}$ is in $\mathcal{K}^\circ(\vec{G}_F)$, then by Theorem 4.17, there exists a circulation $\eta = \{\eta_{ij} \neq 0\}$ on $\vec{G}_F$ satisfying (4.7). Let $m_\ell = |C_\ell| - 1$, then the space of circulations is spanned by vectors

$$\boldsymbol{\eta}_i = \Big[\, \overbrace{0 \ \cdots \ 0}^{\sum_{j=1}^{\ell-1} m_j} \ \boldsymbol{\tau}_\ell \ \overbrace{0 \ \cdots \ 0}^{\sum_{j=\ell+1}^{d} m_j} \ -1 \,\Big] \qquad \text{for } \ell = 1,\ldots,d$$

corresponding to the cycles $C_1,\ldots,C_d$. Therefore, when viewed as a vector, η can be expressed as

$$\boldsymbol{\eta} = \sum_{i=1}^{d} \lambda_i \boldsymbol{\eta}_i = \big[\lambda_1\boldsymbol{\tau}_1 \quad \cdots \quad \lambda_d\boldsymbol{\tau}_d \quad -(\lambda_1 + \cdots + \lambda_d)\big]$$

for some $\lambda_i \in \mathbb{C}^*$ such that $\lambda_1 + \cdots + \lambda_d \neq 0$. We can verify that, along each cycle C_ℓ, we have

$$\frac{\prod_{(i,j)\in\mathcal{E}^+(\vec{C}_\ell)} k_{ij}}{\prod_{(i,j)\in\mathcal{E}^+(\vec{C}_\ell)} \eta_{ij}} = \frac{\prod_{(i,j)\in\mathcal{E}^+(\vec{C}_\ell)} k_{ij}}{\lambda_\ell^{(m_\ell+1)/2}} \quad \text{and} \quad \frac{\prod_{(i,j)\in\mathcal{E}^-(\vec{C}_\ell)} k_{ij}}{\prod_{(i,j)\in\mathcal{E}^-(\vec{C}_\ell)} \eta_{ij}} = \frac{\prod_{(i,j)\in\mathcal{E}^-(\vec{C}_\ell)} k_{ij}}{(-1)^{\frac{m_\ell+1}{2}} \lambda_\ell^{\frac{m_\ell-1}{2}} (\lambda_1 + \cdots + \lambda_d)}$$

the equality between the two (equation (4.7)) thus implies that

$$(-1)^{(m_\ell+1)/2} \frac{\prod_{(i,j)\in\mathcal{E}^+(\vec{C}_\ell)} k_{ij}}{\prod_{(i,j)\in\mathcal{E}^-(\vec{C}_\ell)} k_{ij}} = \frac{\lambda_\ell}{(\lambda_1 + \cdots + \lambda_d)} \quad \text{for } \ell = 1,\ldots,d.$$

Summing over $\ell = 1,\ldots,d$ thus produce the desired equality.

To prove the converse, we adopt the notation

$$P_\ell = \prod_{(i,j)\in\mathcal{E}^+(\vec{C}_\ell)} k_{ij} \qquad N_\ell = \prod_{(i,j)\in\mathcal{E}^-(\vec{C}_\ell)} k_{ij} \qquad t_\ell = (-1)^{|C_\ell|/2} \frac{P_\ell}{N_\ell}$$

for each $\ell = 1, \dots, d$. Assuming $\sum_{\ell=1}^{d} (-1)^{|C_\ell|/2} \frac{P_\ell}{N_\ell} = t_1 + \cdots + t_d = 1$, we want to show that there is a nonzero circulation η on $\vec{G}$ that satisfies (4.7). Let $e \in \mathcal{E}(\vec{G})$ be the shared edge, which is the only edge shared by the cycles, so we have a well-defined assignment $\eta = \{\eta_{ij}\}$, given by

$$\eta_{ij} = \begin{cases} t_\ell & \text{if } e_{ij} \in \mathcal{E}^+(\vec{C}_\ell) \\ -t_\ell & \text{if } e_{ij} \in \mathcal{E}^-(\vec{C}_\ell) \setminus \{e\} \\ -1 & \text{if } (i,j) = e \end{cases}$$

which, by assumption, gives a valid nonzero circulation on $\vec{G}$. Thus, we can verify (4.7) via

$$\prod_{(i,j)\in\mathcal{E}^+(\vec{C}_\ell)} \frac{k_{ij}}{\eta_{ij}} = \frac{P_\ell}{t_\ell^{|C_\ell|/2}} = \frac{P_\ell}{(-1)^{|C_\ell|/2} \frac{P_\ell}{N_\ell} t_\ell^{|C_\ell|/2-1}} = \frac{N_\ell}{(-1)(-t_\ell)^{|C_\ell|/2-1}} = \prod_{(i,j)\in\mathcal{E}^-(\vec{C}_\ell)} \frac{k_{ij}}{\eta_{ij}}.$$

■

Example 4.19 (Simplified balancing condition for Figure 4.3). Through this formulation, the balancing condition given in (4.8) for the digraph shown in Figure 4.3 can be simplified into

$$\frac{k_{50}k_{12}}{k_{52}k_{10}} + \frac{k_{54}k_{32}}{k_{52}k_{34}} = 1.$$

4.4. Examples of global descriptions of exceptional coupling coefficients. The previous section gave an explicit description of the set of exceptional coupling coefficients with respect to a given face F of $\check{\nabla}_G$. The global description of the exceptional coupling coefficients $\mathcal{K}^\circ(G)$ can therefore be obtained as the union of these local contributions from each face. We conclude this section with concrete descriptions of $\mathcal{K}^\circ(G)$ for families of graphs. First, note that many faces of $\check{\nabla}_G$ have no contribution to $\mathcal{K}^\circ(G)$. Combining Theorem 2.3 and Theorem 4.17, we get the following topological constraints on the faces with potentially nontrivial contribution to $\mathcal{K}^\circ(G)$.

Proposition 4.20. *Let Φ be the set of nontrivial proper faces of $\check{\nabla}_G$ with facial subgraphs that are bridgeless and maximally bipartite in their induced subgraphs. Then*

$$\mathcal{K}^\circ(G) = \bigcup_{F\in\Phi} \mathcal{K}^\circ(\vec{G}_F).$$

From this, we can derive a stronger root counting result for networks with no even cycles.

Corollary 4.21. *If G contains no even cycles, then $\vec{f}_{(G,K,\vec{w})}$ is Bernshtein-general, and its number of isolated $\mathbb{C}^*$-zeros, counted with multiplicity, equals the $\operatorname{Vol}(\check{\nabla}_G)$ for any real or complex natural frequencies $\vec{w}$ and any real of complex nonzero coupling coefficients $K = \{k_{ij}\}$.*

In particular, for odd cycles and trees, we can use the results from [11] to derive an exact root count for *any* Kuramoto network.

Corollary 4.22. *If $G = T_N$ is a tree with N nodes then $\vec{f}_{(G,K,\vec{w})}$ has 2^{N-1} $\mathbb{C}^*$-zeros, counting multiplicity, for any choices of real or complex natural frequencies $\vec{w}$ and any choices of real or complex nonzero coupling coefficients $K = \{k_{ij}\}$.*

Corollary 4.23. *If $G = C_N$ is an odd cycle then $\vec{f}_{(G,K,\vec{w})}$ has $N\binom{N-1}{(N-1)/2}$ $\mathbb{C}^*$-zeros, counting multiplicity, for any choices of real or complex natural frequencies $\vec{w}$ and any choices of real or complex nonzero coupling coefficients $K = \{k_{ij}\}$.*

For even cycles, we can explicitly state degeneracy conditions in terms of balanced networks.

Corollary 4.24. *If G is an even cycle, then for any real or complex $\vec{w}$, the following are equivalent:*
1. *the isolated $\mathbb{C}^*$-root count of $\vec{f}_{(G,K,\vec{w})}$, counted with multiplicity, is strictly less than $\operatorname{Vol}(\check{\nabla}_G)$;*
2. *(G,K) has a subnetwork that is balanced with respect to weights K (Definition 4.12).*

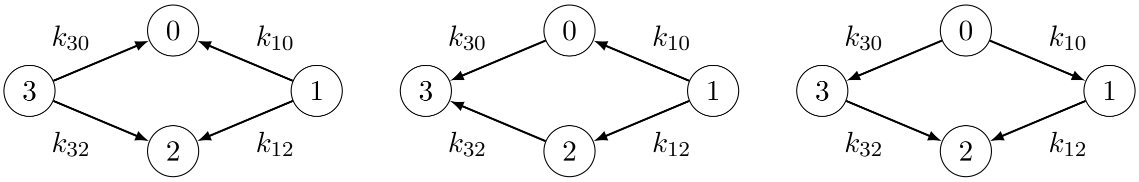

Figure 4.4: Representatives of the classes of balanced subnetworks in C_4

Note that by Lemma 2.1, any result for cycle graphs extends to *unicycle graphs*, i.e. graphs that contain a unique cycle.

Example 4.25 (The 4-cycle case). Consider the case of $G = C_4$. As shown in [11, Theorem 16] and Theorem 3.5, for generic choices of $\vec{w}$ and K, $\vec{f}_G$ has 12 $\mathbb{C}^*$-zeros. This is the adjacency polytope bound. With the choice of $\vec{w}$ remain generic, we will illustrate the conditions given Corollary 4.24. C_4 has up to 6 balanced subnetworks supported by the digraphs shown in Figure 4.4 and their transposes. With these, we have the following decomposition of the coupling coefficients:

1. Consider the 1-dimensional "balancing variety" defined by the binomial system

$$\begin{cases} k_{10}k_{12}k_{32}^{-1}k_{30}^{-1} = 1 \\ k_{10}k_{12}^{-1}k_{32}^{-1}k_{30} = 1 \\ k_{10}k_{12}^{-1}k_{32}k_{30}^{-1} = 1, \end{cases} \tag{4.10}$$

which will produce all 6 balanced subnetworks. It can be parameterized by

$$k_{10} = k_{12} = k_{32} = k_{30} = s,$$

for $s \in \mathbb{C}^*$. Numerical computation shows that generic choice of $s \in \mathbb{C}^*$ produces an algebraic Kuramoto system $\vec{f}_G$ with only 6 $\mathbb{C}^*$-zeros. Moreover, taking $s = 1$ and $w_1 = 1.1, w_2 = -2.1, w_3 = 1$, all six $\mathbb{C}^*$-zeros can be *real*

2. There are three 2-dimensional balancing varieties, all containing the 1-dimensional variety defined in (4.10), which are defined by two out of the three equations from this system, i.e.,

$$\begin{cases} k_{10}k_{12}k_{32}^{-1}k_{30}^{-1} = 1 \\ k_{10}k_{12}^{-1}k_{32}^{-1}k_{30} = 1 \end{cases} \quad \text{or} \quad \begin{cases} k_{10}k_{12}^{-1}k_{32}^{-1}k_{30} = 1 \\ k_{10}k_{12}^{-1}k_{32}k_{30}^{-1} = 1, \end{cases} \quad \text{or} \quad \begin{cases} k_{10}k_{12}k_{32}^{-1}k_{30}^{-1} = 1 \\ k_{10}k_{12}^{-1}k_{32}k_{30}^{-1} = 1, \end{cases}$$

each producing 4 balanced subnetworks. The first, for example, can be parameterized as

$$k_{10} = s \qquad k_{12} = t \qquad k_{32} = \pm t \qquad k_{30} = \pm s \qquad \text{for } (s,t) \in (\mathbb{C}^*)^2.$$

The other two can be parameterized similarly. Numerical computations suggest that generic (s,t) produce algebraic Kuramoto systems having 8 solutions. Moreover, taking $s = 1, t = -1.001, w_1 = 1.1, w_2 = -2.1, w_3 = 1$ all 8 solutions can be real.

3. There are three 3-dimensional balancing varieties defined by binomial equations

$$k_{10}k_{12}k_{32}^{-1}k_{30}^{-1} = 1 \qquad k_{10}k_{12}^{-1}k_{32}^{-1}k_{30} = 1 \qquad k_{10}k_{12}^{-1}k_{32}k_{30}^{-1} = 1,$$

each producing 2 balanced subnetworks. The first of the three can be parameterized by

$$k_{10} = s \qquad k_{12} = u/s \qquad k_{32} = t \qquad k_{30} = u/t,$$

for $(s,t,u) \in (\mathbb{C}^*)^3$. The other two can be parameterized similarly. Numerical experiments show that a generic choice of coupling coefficients on one of these varieties gives 10 $\mathbb{C}^*$-zeros. Moreover, with $u = 1.01, s = 1, t = -1.001, w_1 = 1.1, w_2 = -2.1, w_3 = 1$, all zeros are real.

4. The remaining choices of K, form a Zariski-dense subset in the space of all coupling coefficients for C_4, and define an algebraic Kuramoto system with 12 $\mathbb{C}^*$-zeros.

Under the assumption that $\vec{w}$ is generic, there are no other possibilities. Interestingly, with special choices of $\vec{w}$, the same conditions on exceptional coupling coefficients will produce positive-dimensional solutions. This behavior is explored in Example 5.4.

Example 4.26. We now consider a graph G formed as two 4-cycles sharing one edge as in Figure 4.3. The geometry of the adjacency polytope for this and similar graphs was studied in detail by D'Ali, Delucchi, and Michałek [15] and the related work [12]. By treating each cycle as a copy of C_4, the equations from Example 4.25 with respect to the cycles on vertices $\{v_0, v_1, v_2, v_5\}$ and $\{v_2, v_3, v_4, v_5\}$ apply here as well. In addition, 9 equations define other patches of $\mathcal{K}^\circ(G)$:

$$\begin{aligned}
&\frac{k_{50}k_{12}}{k_{52}k_{10}} + \frac{k_{54}k_{32}}{k_{52}k_{34}} = 1\,, &&\frac{k_{50}k_{12}}{k_{52}k_{10}} + \frac{k_{43}k_{32}}{k_{52}k_{45}} = 1\,, &&\frac{k_{50}k_{12}}{k_{52}k_{10}} + \frac{k_{54}k_{43}}{k_{52}k_{23}} = 1\,,\\
&\frac{k_{01}k_{12}}{k_{52}k_{05}} + \frac{k_{54}k_{32}}{k_{52}k_{34}} = 1\,, &&\frac{k_{01}k_{12}}{k_{52}k_{05}} + \frac{k_{43}k_{32}}{k_{52}k_{45}} = 1\,, &&\frac{k_{01}k_{12}}{k_{52}k_{05}} + \frac{k_{54}k_{43}}{k_{52}k_{23}} = 1\,,\\
&\frac{k_{01}k_{50}}{k_{52}k_{12}} + \frac{k_{54}k_{32}}{k_{52}k_{34}} = 1\,, &&\frac{k_{01}k_{50}}{k_{52}k_{12}} + \frac{k_{43}k_{32}}{k_{52}k_{45}} = 1\,, &&\frac{k_{01}k_{50}}{k_{52}k_{12}} + \frac{k_{54}k_{43}}{k_{52}k_{23}} = 1.
\end{aligned}$$

They corresponds to the 9 transpose-pairs of maximally bipartite balanced digraphs in G, and each defines a subset of exceptional coupling coefficients of co-dimension 1.

5. Positive-dimensional solutions for homogeneous networks.

The previous section explored structure of the exceptional coupling coefficients. We now turn our attention to the interesting role played by the natural frequencies $\vec{w}$. Indeed positive-dimensional zero sets for the algebraic Kuramoto equations that can appear when both K and $\vec{w}$ are chosen to be special values. They represent synchronization configurations that have at least one degree of freedom (even after fixing a rotational frame). In this section, we add to the existing literature on constructions of positive-dimensional zero sets for the Kuramoto equations [1, 14, 20, 29, 35] and characterize conditions under which they arise. We focus on the most widely studied case of homogeneous oscillators, i.e., $\vec{w} = w\vec{1}$ for some real or complex constant w. They correspond to Kuramoto systems (2.3) with zero constant terms. Therefore, without loss of generality we will fix $w_i = 0$ for each $i = 0, \ldots, n$ in this section and use the notation $(G, K, \vec{0})$ for a Kuramoto network of homogeneous oscillators.

It is worth reiterating that positive-dimensional $\mathbb{C}^*$-zero sets for the algebraic Kuramoto system can only occur when when the vector of coupling coefficients is in the set of exceptional coupling coefficients and hence the system is not Bernshtein-general.

Corollary 5.1. *For a connected graph G, if the $\mathbb{C}^*$-zero set of the algebraic Kuramoto system $\vec{f}_{(G,K)}$ is positive-dimensional, then $K \in \mathcal{K}^\circ(G)$.*

Under the assumption that the oscillators are homogeneous, we now study the additional topological and algebraic conditions that guarantee the existence of positive-dimensional zero sets.

We start our investigation with bipartite networks for which positive-dimensional solutions can be constructed as restrictions of tree solutions (Definition 4.7) derived from certain facet subdigraphs. This is because when G is bipartite, Theorem 2.3 gives that G itself is a facet subgraph, i.e., there exists a $F \in \mathcal{F}(\check{\nabla}_G)$ such that $G = G_F$. In this case, $\check{\nabla}_G = \{0\} \cup F \cup (-F)$. That is, F and $-F$ contain the exponent vectors of all terms, and then the algebraic Kuramoto system can be expressed in the simple form

$$\vec{f}_G(\boldsymbol{x}) = -\check{Q}(\vec{G}_F)(\boldsymbol{x}^{\check{Q}(\vec{G}_F)} \circ \boldsymbol{a}(G))^\top + \check{Q}(\vec{G}_F)(\boldsymbol{x}^{-\check{Q}(\vec{G}_F)} \circ \boldsymbol{a}(G))^\top. \tag{5.1}$$

Note that the two terms are the circulation forms of $\operatorname{init}_F(\vec{f}_G^*)$ and $\operatorname{init}_{-F}(\vec{f}_G^*)$, respectively.

In the previous section, we constructed tree solutions (Definition 4.7) for which the first term of (5.1) vanishes under the assumption that $K \in \mathcal{K}^\circ(G)$. Our strategy now is to impose additional topological and algebraic conditions so that the second term of (5.1) also vanishes, and then the tree solution parameterizes a positive-dimensional solution for the entire system. Of course, this strategy is unlikely going to parameterize the entire positive-dimensional solution set. But, as we will demonstrate, it is applicable for a surprisingly large family of graphs.

5.1. Cycles. We first consider cycle networks. In this context, Corollary 4.24 can be paraphrased as the following necessary condition for the existence of positive-dimensional zero sets.

Proposition 5.2. *Let $G = C_N$. If, for a choice of K and $\vec{w}$, the $\mathbb{C}^*$-zero sets of $\vec{f}_{(G,K,\vec{w})}$ is positive-dimensional, then N is even and (G,K) contains a balanced subnetwork (Definition 4.12).*

We now show that with the additional assumptions that the oscillators are homogeneous and the coupling coefficients on edges are among $\{\pm k\}$ for a $k \neq 0$, the converse is also true.

Proposition 5.3 (Non-isolated $\mathbb{C}^*$-zero set for even cycles). *Let $G = C_N$ for an even $N > 2$. Then there exists a choice of coupling coefficients K for which the algebraic Kuramoto system $\vec{f}_{(G,K,w\vec{1})}$ has infinitely many $\mathbb{C}^*$-solutions. Specifically, for a fixed $k \in \mathbb{C}^*$ any choice of $k_{ij} \in \{\pm k\}$ with*
- *an even number of negative choices if $N \equiv 0 \mod 4$,*
- *an odd number of negative choices if $N \equiv 2 \mod 4$,*

the $\vec{f}_{(G,K,\vec{0})}$ derived from a homogeneous network has a positive-dimensional $\mathbb{C}^*$-zero set, which contains the image of $\boldsymbol{x}_{\vec{T}}$ (Definition 4.7), for $\vec{T} < G$. Moreover, if $k \in \mathbb{R} \setminus \{0\}$, the corresponding transcendental Kuramoto system has a positive-dimensional real zero set.

Note that the conditions given here can be stated more succinctly: It is equivalent to saying G contains a balanced subnetwork and the coupling coefficients are among $\{\pm k\}$.

Proof. Let $\vec{H}$ be an balanced subdigraph (Definition 4.11) of C_N. Then the assumption ensures that $\vec{H}$ is balanced with respect to K.

Fix any weak spanning tree $\vec{T}$ of $\vec{H}$ and let $\boldsymbol{x}_{\vec{T}}$ be the induced tree solution defined in Definition 4.7. With a straightforward calculation, we verify

$$\check{Q}(\vec{H})\left(\boldsymbol{x}_{\vec{T}}(\lambda)^{-\check{Q}(\vec{H})} \circ \boldsymbol{a}(\vec{H})\right)^{\top} = \check{Q}(\vec{H})\left((\lambda \cdot \boldsymbol{\eta} \circ \boldsymbol{a}(\vec{H}))^{-I} \circ \boldsymbol{a}(\vec{H})\right)^{\top} = \check{Q}(\vec{H})\left(-\frac{k^2}{4\lambda} \cdot \boldsymbol{\eta}\right)^{\top} = \vec{0}.$$

Combined with the calculation above, we see that $\vec{f}_G(\boldsymbol{x}(\lambda)) = \vec{0}$ for all $\lambda \in \mathbb{C}^*$ and thus the $\mathbb{C}^*$-zero set of $\vec{f}_G = \vec{0}$ is positive-dimensional.

Finally, by restricting $\lambda \in \mathbb{C}^*$ to the unit circle S^1, and $k \in \mathbb{R}$, the $\mathbb{C}^*$-orbit constructed here produces a 1-dimensional real zero set to the original transcendental Kuramoto system (2.2). ∎

Example 5.4 (4-cycle, again). For $G = C_4$, as noted in Example 4.25, there can be as many as 6 balanced subnetworks, depending on the choices of coupling coefficients. They come in three pairs corresponding to reversing the orientation of all arcs. A representative of each pair is shown in Figure 4.4. Each pair of balanced subnetworks produces an one-dimensional $\mathbb{C}^*$-zero set of $\vec{f}_G$ through the formula given in Proposition 5.3.

1. Consider the first subdigraph $\vec{H}_1$ in Figure 4.4. It is balanced if $k_{10}k_{32} = k_{12}k_{30}$. Then with the choice of $\vec{T}_1$ having arcs $(1,0),(1,2),(3,0)$, we can compute

$$\check{Q}(\vec{T}_1) = \begin{bmatrix} +1 & +1 & 0 \\ 0 & -1 & 0 \\ 0 & 0 & +1 \end{bmatrix} \qquad \check{Q}(\vec{T}_1)^{-1} = \begin{bmatrix} +1 & +1 & 0 \\ 0 & -1 & 0 \\ 0 & 0 & +1 \end{bmatrix} \qquad \boldsymbol{\eta}_{\vec{T}_1} = \begin{bmatrix} -1 & +1 & +1 \end{bmatrix},$$

where the notation is as in Proposition 5.3. Then the function $\boldsymbol{x} : \mathbb{C}^* \to (\mathbb{C}^*)^3$, given by

$$\boldsymbol{x}(\lambda) = (\lambda \cdot \boldsymbol{\eta}_{\vec{T}_1} \circ \begin{bmatrix} a_{10} & a_{12} & a_{30} \end{bmatrix}^{-I})^{\check{Q}(\vec{T}_1)^{-1}} = \begin{bmatrix} -\frac{2\mathrm{i}\lambda}{k_{10}} & -\frac{k_{12}}{k_{10}} & \frac{2\mathrm{i}\lambda}{k_{30}} \end{bmatrix}$$

has image inside the $\mathbb{C}^*$-zero set of $\vec{f}_{C_4}$. In other words, the function

$$\boldsymbol{x}(\lambda) = \begin{bmatrix} -2\mathrm{i}\lambda/k_{10} & -k_{12}/k_{10} & +2\mathrm{i}\lambda/k_{30} \end{bmatrix} \qquad \text{if} \quad k_{10}k_{32} = k_{12}k_{30}$$

parameterizes the open part of an one-dimensional orbit in the $\mathbb{C}^*$-zero set of $\vec{f}_{C_4}$. In the special case when $k_{ij} = 1$, this one-dimensional orbit is *balanced* in the sense of [35, Definition 3.1] and [35] provides analysis of the stability and geometry of such orbits.

2. The second subnetwork $\vec{H}_2$ in Figure 4.4 is balanced if $k_{10}k_{30} = k_{12}k_{23}$. With $\vec{T}_2 < \vec{H}_2$ given by arcs $(1,0),(1,2),(0,3)$ and by following the construction above, we have

$$\boldsymbol{x}(\lambda) = \begin{bmatrix} +2\mathrm{i}\lambda/k_{10} & -k_{12}/k_{10} & +k_{03}/2\mathrm{i}\lambda \end{bmatrix} \qquad \text{if} \quad k_{10}k_{30} = k_{12}k_{23}$$

whose image is in the $\mathbb{C}^*$-zero set of $\vec{f}_{C_4}$ for any $\lambda \in \mathbb{C}^*$. Note that even in the special case of $k_{ij} = 1$, this orbit is *not* balanced (in the sense of [35, Definition 3.1]) for $\lambda \neq 1$.

3. Finally, the third subnetwork $\vec{H}_3$ in Figure 4.4 is balanced if $k_{10}k_{12} = k_{32}k_{03}$. With the choice $\vec{T}_3 < \vec{H}_3$, and following the construction above, we have

$$\boldsymbol{x}(\lambda) = \begin{bmatrix} +k_{01}/2\mathrm{i}\lambda & -k_{01}k_{12}/4\lambda^2 & -k_{03}/2\mathrm{i}\lambda \end{bmatrix} \quad \text{if} \quad k_{10}k_{12} = k_{32}k_{30}$$

whose image is in the $\mathbb{C}^*$-zero set of $\vec{f}_{C_4}$ for any $\lambda \in \mathbb{C}^*$. This orbit is more interesting as all three complex phase variables x_1, x_2, x_3 are nonconstant relative to the reference phase $x_0 = 1$. It is also *not* balanced (in the sense of [35, Definition 3.1]).

Moreover, if the coupling coefficients satisfy the condition $\boldsymbol{k}^2(C_4) = c^2 \cdot \mathbf{1}$ for some $c \in \mathbb{R}$, then each of the three $\mathbb{C}^*$-orbits contains a one-real-dimensional components in the real torus $(S^1)^3$. Indeed, by the restriction $\lambda = \frac{ce^{\mathrm{i}t}}{2\mathrm{i}}$, the three orbits constructed above reduce to parameterized zero sets of one real-dimension inside the real torus. If we define

$$\sigma^{ij}_{\ell m} = \begin{cases} 0 & \text{if } k_{ij}/k_{\ell m} > 0 \\ \pi & \text{otherwise,} \end{cases} \qquad \text{and} \quad \sigma^{ij} = \begin{cases} 0 & \text{if } k_{ij} > 0 \\ \pi & \text{otherwise,} \end{cases}$$

then the three potential real orbits can be expressed as

$$\begin{cases} \theta_1 = t + \pi + \sigma^{10} \\ \theta_2 = \pi + \sigma^{12}_{10} \\ \theta_3 = t + \sigma^{30} \end{cases} \text{if } \frac{k_{10}k_{32}}{k_{12}k_{30}} = 1, \quad \begin{cases} \theta_1 = \sigma^{10} + t \\ \theta_2 = \pi + \sigma^{21}_{10} \\ \theta_3 = \sigma^{30} - t \end{cases} \text{if } \frac{k_{10}k_{30}}{k_{12}k_{23}} = 1, \quad \begin{cases} \theta_1 = \sigma^{10} - t \\ \theta_2 = \sigma^{21}_{10} - 2t \\ \theta_3 = \pi + \sigma^{30} - t \end{cases} \text{if } \frac{k_{10}k_{12}}{k_{32}k_{30}} = 1,$$

with $\theta_0 = 0$. It is easy to see if k_{ij}'s are identical, then all three real orbits exist. Moreover, these three orbits intersects at a singular point $(\theta_0, \theta_1, \theta_2, \theta_3) = (0, \pi/2, \pi, \pi/2)$. These positive-dimensional solution sets have been studied in [20, 29, 35]. In particular, [35, Section 5.2] provides a topological analysis for the orbits. In Example 5.4, we showed they can also be derived systematically from balanced subnetworks.

5.2. Multiple even cycles sharing one edge.

We now show that $\vec{f}_G$ can have positive-dimensional zero sets if G is a graph consisting of multiple even cycles sharing a single edge (e.g., Figure 5.1a).

Proposition 5.5. *Suppose G consists of d independent even cycles $C_1, \ldots, C_d$ that share a single edge e, then with the choice of the coupling coefficients*

$$k_{ij} = \begin{cases} sd & \text{if } \{i,j\} = e \\ s & \text{otherwise,} \end{cases}$$

for any $s \in \mathbb{C}^*$, and homogeneous natural frequencies $\vec{w} = w \cdot \vec{1}$ for any $w \in \mathbb{C}^*$, the algebraic Kuramoto system $\vec{f}_G$ derived from the network $(G, K, w \cdot \vec{1})$ has a positive-dimensional $\mathbb{C}^*$-zero set.

Proof. Since G is bipartite, by Theorem 2.3, there exists a facet F of $\check{\nabla}_G$ such that $G_F = G$, and thus $\check{\nabla}_G = \{\vec{0}\} \cup F \cup (-F)$. Consequently,

$$\vec{f}_G(\boldsymbol{x}) = \check{Q}(\vec{G}_F)(\boldsymbol{x}(\lambda)^{\check{Q}(\vec{G}_F)} \circ \boldsymbol{a}(\vec{G}_F))^\top + \check{Q}(\vec{G}_{-F})(\boldsymbol{x}(\lambda)^{\check{Q}(\vec{G}_{-F})} \circ \boldsymbol{a}(\vec{G}_{-F}))^\top.$$

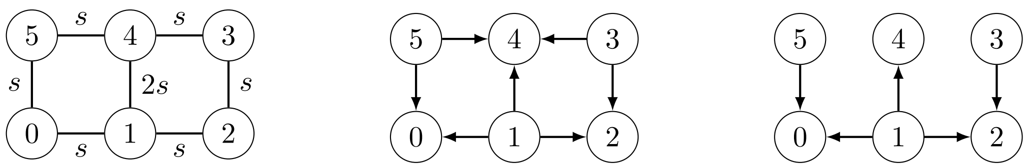

(a) G (b) A facet subdigraph $\vec{G}_F$ (c) $\vec{T}$ inside $\vec{G}_F$

Figure 5.1: A network with two independent even cycles.

Let T be a spanning tree of G that contains e, and let $\vec{T}$ be the corresponding subdigraph such that $\vec{T} < \vec{G}_F$. Consider the tree solution (Definition 4.7)

$$\boldsymbol{x}_{\vec{T}}(\lambda_1, \dots, \lambda_d) = \left[\left(\sum_{k=1}^{d} \lambda_k \boldsymbol{\tau}_k \right) \circ \boldsymbol{a}_{\vec{T}}^{-I} \right]^{\check{Q}(\vec{T})^{-1}}$$

where each vector $\boldsymbol{\tau}_k$ contains coefficients with which an edge in $\mathcal{E}(\vec{H}) \setminus \mathcal{E}(\vec{T})$ can be written as a linear combination of edges in $\vec{T}$. To prove the existence of positive-dimensional components, it is sufficient to restrict our attention to the case $\lambda = \lambda_1 = \ldots = \lambda_d$, i.e., the nonconstant function

$$\boldsymbol{x}(\lambda) := \boldsymbol{x}_{\vec{T}}(\lambda, \dots, \lambda) = \left[\lambda \left(\sum_{k=1}^{d} \boldsymbol{\tau}_k \right) \circ \boldsymbol{a}_{\vec{T}}^{-I} \right]^{\check{Q}(\vec{T})^{-1}} = \left[\lambda \cdot \boldsymbol{\eta}_{\vec{T}} \circ \boldsymbol{a}_{\vec{T}}^{-I} \right]^{\check{Q}(\vec{T})^{-1}}$$

in which the first $n-1$ entries of $\boldsymbol{\eta}_{\vec{T}}$ are ± 1, and its n-th entry is $\pm d$. By Proposition 4.18,

$$\check{Q}(\vec{G}_F)(\boldsymbol{x}(\lambda)^{\check{Q}(\vec{G}_F)} \circ \boldsymbol{a}(\vec{G}_F))^\top = \vec{0} \quad \text{for any } \lambda \in \mathbb{C}^*.$$

It remains to show $\check{Q}(\vec{G}_{-F})(\boldsymbol{x}(\lambda)^{\check{Q}(\vec{G}_{-F})} \circ \boldsymbol{a}(\vec{G}_{-F}))^\top = \vec{0}$. Since $\boldsymbol{a}(\vec{T}) = \frac{\boldsymbol{k}(\vec{T})}{2\mathrm{i}} = [\, s \ \cdots \ s \ sd \,]$,

$$\boldsymbol{x}(\lambda)^{-\check{Q}(\vec{T})} \circ \boldsymbol{a}(\vec{T}) = (\lambda \cdot \boldsymbol{\eta}_{\vec{T}} \circ \boldsymbol{a}(\vec{T})^{-I})^{-I} \circ \boldsymbol{a}(\vec{T}) = \lambda^{-1} \boldsymbol{\eta}_{\vec{T}}^{-I} \circ \left[\tfrac{s^2}{-4} \ \cdots \ \tfrac{s^2}{-4} \ \tfrac{s^2 d^2}{-4} \right] = \frac{s^2}{-4\lambda} \boldsymbol{\eta}_{\vec{T}}$$

Moreover, by construction, $\boldsymbol{x}(\lambda)^{\vec{v}_i} \cdot \boldsymbol{a}(e_i) = \lambda u_i$ for $i = 1, \dots, d$. Therefore,

$$\boldsymbol{x}(\lambda)^{-\vec{v}_i} \cdot \boldsymbol{a}(e_i) = \lambda^{-1} \boldsymbol{a}^2(e_i) u_i^{-1} = \frac{s^2}{-4\lambda} u_i,$$

since $u_1 \in \{\pm 1\}$. This shows that

$$\boldsymbol{x}(\lambda)^{\check{Q}(\vec{G}_{-F})} \circ \boldsymbol{a}(\vec{G}_{-F}) = \left[\boldsymbol{x}(\lambda)^{-\check{Q}(\vec{T})} \circ \boldsymbol{a}(\vec{T}) \quad \boldsymbol{x}(\lambda)^{-\vec{v}_1} \cdot \boldsymbol{a}(e_1) \quad \boldsymbol{x}(\lambda)^{-\vec{v}_2} \cdot \boldsymbol{a}(e_1) \right] = \frac{s^2}{-4\lambda} \boldsymbol{\eta}.$$

Consequently, $\vec{f}_G(\boldsymbol{x}(\lambda)) = \vec{0}$ for any $\lambda \in \mathbb{C}^*$, i.e., the $\mathbb{C}^*$-zero set of $\vec{f}_G$ is positive-dimensional. ■

Example 5.6. Consider the network shown in Figure 5.1a. We fix the facet

$$F = \operatorname{conv}\{\vec{e}_1, \vec{e}_1 - \vec{e}_2, \vec{e}_1 - \vec{e}_4, \vec{e}_3 - \vec{e}_2, \vec{e}_3 - \vec{e}_4, \vec{e}_5 - \vec{e}_4, \vec{e}_5\} \subset \mathbb{R}^5$$

whose facet subdigraph is shown in Figure 5.1b. We also fix a choice of $\vec{T} < \vec{G}_F$ shown in Figure 5.1c. With this choice and the ordering of the arcs $(1,0)$, $(1,2)$, $(3,2)$, $(5,0)$, $(1,4)$, $(3,4)$, $(5,4)$, we have

$$\check{Q}(\vec{T}) = \begin{bmatrix} 1 & 1 & 0 & 0 & 1 \\ 0 & -1 & -1 & 0 & 0 \\ 0 & 0 & 1 & 0 & 0 \\ 0 & 0 & 0 & 0 & -1 \\ 0 & 0 & 0 & 1 & 0 \end{bmatrix}, \qquad \check{Q}(\vec{T})^{-1} = \begin{bmatrix} 1 & 1 & 1 & 1 & 0 \\ 0 & -1 & -1 & 0 & 0 \\ 0 & 0 & 1 & 0 & 0 \\ 0 & 0 & 0 & 0 & 1 \\ 0 & 0 & 0 & -1 & 0 \end{bmatrix}, \qquad \vec{\eta}_1 = \begin{bmatrix} 0 \\ -1 \\ +1 \\ 0 \\ +1 \\ -1 \\ 0 \end{bmatrix}, \qquad \vec{\eta}_2 = \begin{bmatrix} -1 \\ 0 \\ 0 \\ +1 \\ +1 \\ 0 \\ -1 \end{bmatrix}.$$

We also define:

$$\boldsymbol{\eta} = \vec{\eta}_1^\top + \vec{\eta}_2^\top = \begin{bmatrix} -1 & -1 & +1 & +1 & +2 & -1 & -1 \end{bmatrix} \quad \text{and} \quad \boldsymbol{\eta}_T = \begin{bmatrix} -1 & -1 & +1 & +1 & +2 \end{bmatrix}.$$

We then verify that the construction $\boldsymbol{x}(\lambda) = (\lambda \cdot \boldsymbol{\eta}_T \circ \boldsymbol{a}(\vec{T})^{-I})^{\check{Q}(\vec{T})^{-1}}$ above produces

$$(\lambda \begin{bmatrix} -1 & -1 & +1 & +1 & +2 \end{bmatrix} \circ \begin{bmatrix} \frac{s}{2\mathrm{i}} & \frac{s}{2\mathrm{i}} & \frac{s}{2\mathrm{i}} & \frac{s}{2\mathrm{i}} & \frac{2s}{2\mathrm{i}} \end{bmatrix}^{-I})^{\check{Q}(\vec{T})^{-1}} = \begin{bmatrix} -\frac{2\mathrm{i}\lambda}{s} & +1 & +\frac{2\mathrm{i}\lambda}{s} & -1 & +\frac{2\mathrm{i}\lambda}{s} \end{bmatrix},$$

which parameterizes a one-dimensional $\mathbb{C}^*$-zero of $\vec{f}_G$. Moreover, by choosing $\lambda(t) = \frac{se^{\mathrm{i}t}}{2\mathrm{i}}$, $\boldsymbol{x} \in (S^1)^5$ for any $t \in \mathbb{R}$, $\log(\boldsymbol{x})$ produces the one-dimensional real zero set

$$(\theta_0, \theta_1, \theta_2, \theta_3, \theta_4, \theta_5) = (0, t+\pi, 0, t, \pi, t)$$

for the transcendental Kuramoto system (2.2) derived from the network in Figure 5.1a.

5.3. Homogeneous networks with uniform coupling coefficients. We now consider the special case of networks with uniform coupling coefficients (k_{ij} are all identical). Without loss of generality, we fix $k_{ij} = 1$ and use the notation $(G, \mathbf{1}, \vec{0})$ to denote such a homogeneous and uniform network. In this case, the conditions for the exceptionality of coupling coefficients and the existence of positive-dimensional zero sets become topological constraints. We conclude this section by listing a few families of graphs on which a homogeneous Kuramoto network with uniform coupling coefficients has a positive-dimensional set of synchronization configurations.

$G = C_{4m}$ for an integer $m \geq 1$ is a sufficient condition for having a positive-dimensional zero set. Its existence was first established in [29]. From the framework developed in this paper, we can also construct such a 1-dimensional curve in the solution set using Proposition 5.3, since $(C_{4m}, \mathbf{1}, \vec{0})$ is a balanced cycle. Interestingly, this particular positive-dimensional zero set, derived from C_{4m}, can be extended directly to a large family of networks.

Proposition 5.7. *Suppose G contains a cycle $C = C_{4m}$ for an $m \geq 2$. Let $V^+ \cup V^- = \mathcal{V}(C)$ be the partition of C as a bipartite graph. If any path in G connecting nodes in V^+ and V^- includes at least one edge in C then $\vec{f}_{(G,\mathbf{1},\vec{0})}$ has a positive-dimensional $\mathbb{C}^*$-zero set. Moreover, the corresponding transcendental Kuramoto system has a positive-dimensional real zero set.*

Proof. Without loss of generality, we can assume that node 0 is in C and $0 \in V^-$. According to Proposition 5.3, there is a 1-dimensional solution to the subsystem $\vec{f}_{(C,\mathbf{1},\vec{0})}$ given by

$$x_i(\lambda) = \begin{cases} \pm\lambda & \text{if } i \in V^+ \\ \pm 1. & \text{if } i \in V^- \end{cases}$$

where the signs depends the choice of the weak spanning tree of C from which this is derived.

By assumption, each node outside C is either connected to nodes in V^+ or V^- through edges outside C. We label these two sets of nodes as U^+ and U^- respectively, and we define

$$x_i(\lambda) = \begin{cases} \lambda & \text{if } i \in U^+ \\ 1. & \text{if } i \in U^- \end{cases}$$

Then in both cases of $i, j \in U^+ \cup V^+$ and or $i, j \in U^- \cup V^-$, we have

$$\frac{x_i}{x_j} - \frac{x_j}{x_i} = (\pm 1) - (\pm 1) = 0.$$

Recall that polynomials $\vec{f}_{(G,\mathbf{1},\vec{0})}$ are sums or differences between polynomials in $\vec{f}_{(C,\mathbf{1},\vec{0})}$ and $\frac{x_i}{x_j} - \frac{x_j}{x_i}$ for edges $\{i, j\}$ in $\mathcal{E}(G) \backslash \mathcal{E}(C)$, which, by assumption, must be incident to nodes only in $U^+ \cup V^+$ or $U^- \cup V^-$. Therefore, $(x_1(\lambda), \dots, x_n(\lambda))$ defines a curve in the $\mathbb{C}^*$-zero set of $\vec{f}_{(G,\mathbf{1},\vec{0})}$.

Finally, by restricting λ to the unit circle S^1, i.e., setting $\lambda = e^{\mathrm{i}\theta}$ for $\theta \in \mathbb{R}$, we get a curve of in the real zero set of the transcendental Kuramoto system. ∎

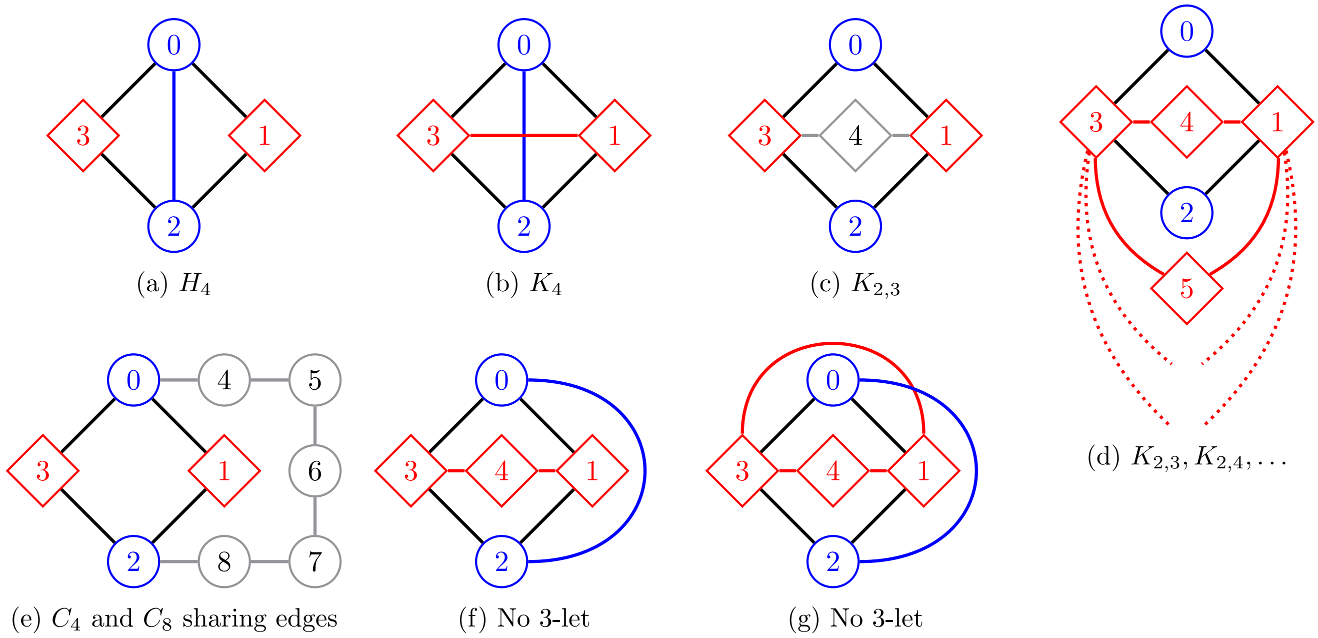

Figure 5.2: Examples of homogeneous and uniform networks into which a solution curve derived from C_4 can be lifted according to Proposition 5.7. Nodes in V^+, V^-, U^+, U^- are represented by red diamonds, blue circles gray diamonds, and gray circles respectively.

Example 5.8 (Extending C_4 solutions). With this result, we can extend the 1-dimensional $\mathbb{C}^*$-zero set for the Kuramoto system derived from a cycle network of 4 homogeneous oscillators with uniform coupling coefficients directly to other networks. Figure 5.2 shows some of the examples of networks to which such extension is possible. This result gives us 1-dimensional curves

$$\boldsymbol{x}_{(\mathrm{a})}(\lambda) = \begin{bmatrix} -\lambda & -1 & \lambda \end{bmatrix} \qquad \boldsymbol{x}_{(\mathrm{b})}(\lambda) = \begin{bmatrix} -\lambda & -1 & \lambda \end{bmatrix}$$
$$\boldsymbol{x}_{(\mathrm{c})}(\lambda) = \begin{bmatrix} -\lambda & -1 & \lambda & \lambda \end{bmatrix} \qquad \boldsymbol{x}_{(\mathrm{e})}(\lambda) = \begin{bmatrix} -\lambda & -1 & \lambda & 1 & 1 & 1 & 1 & 1 \end{bmatrix}$$

in their respective $\mathbb{C}^*$-zero sets (as well as real zero sets via the restriction $\lambda = e^{\mathrm{i}\theta}$). This shows that the respective system have positive-dimensional zero sets.

The graph $K_{2,3}$ in Figure 5.2c is a complete bipartite graph, which consists of all edges between two sets of nodes ($\{1,3\}$ and $\{0,2,4\}$, in this case). The construction in Proposition 5.7 extends trivially to $K_{2,m}$ for $m \geq 2$, since $K_{2,m}$ can be created from C_4 by adding nodes $4, \ldots, m+1$ and edges $\{1, j\}$ and $\{3, j\}$ for $j = 5, \ldots,$ as in Figure 5.2d.

Corollary 5.9. *For any $m \geq 2$, $\vec{f}_{(K_{2,m}, \mathbf{1}, \vec{0})}$ has a positive-dimensional $\mathbb{C}^*$-zero set, and the corresponding transcendental Kuramoto system has a positive-dimensional real zero set.*

Example 5.10 (Beyond 3-lets). The example $K_{2,3}$ (Figure 5.2c) is noteworthy for another reason: It is an example of a graph that contains a *3-let*, i.e., a set of 3 nodes ($\{0,2,4\}$ in this case) sharing the same set of neighbors. In [20, Corollary 2.9] Harrington, Schenck, and Stillman showed that the Kuramoto system derived from a homogeneous and uniform Kuramoto network based on a 2-connected graph that contains a 3-let must have a positive-dimensional zero set. Figures 5.2f and 5.2g shows graphs obtained by adding edges to $K_{2,3}$, which no longer contain 3-lets. However, Proposition 5.7 shows that there are still positive-dimensional $\mathbb{C}^*$-zero sets. Indeed, the curve

$$\boldsymbol{x}(\lambda) = \begin{bmatrix} -\lambda, -1, \lambda, \lambda \end{bmatrix}$$

is contained in the $\mathbb{C}^*$-zero sets of the Kuramoto systems derived from all three homogeneous and uniform networks despite the extra terms introduced by the added edges.

Example 5.11. Similarly, starting with C_8, Proposition 5.7 shows that the 1-dimensional curve

$$\boldsymbol{x}(\lambda) = \begin{bmatrix} -\lambda & -1 & \lambda & 1 & -\lambda & -1 & \lambda \end{bmatrix} \tag{5.2}$$

can be embedded into the zero set of the Kuramoto system derived from the network in Figure 5.3a.

We end with the observation that for simplicity the conditions in Proposition 5.7 is made too restrictive. For instance, even though the network in Figure 5.3b does not satisfy the condition in this proposition, the solution (5.2) is still a valid curve solution to the derived Kuramoto system. This implies that 1-dimensional cycle solutions can be extended to a much broader class of networks.

6. Concluding remarks. We studied the structure of the zero sets of the Kuramoto equations and its algebraic counterpart. By leveraging a recently discovered three-way connection between the graph-theoretic, convex-geometric, and tropical view points, we answered three key questions.

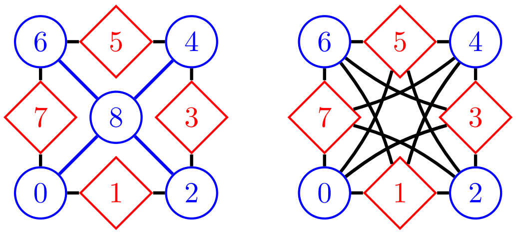

(a) Adding edges to C_8 (b) Adding more edges

Figure 5.3: Examples of homogeneous and uniform networks to which a cycle solution derived from C_8 can be lifted into.

For Question 1.1, we showed that *for generic natural frequencies and generic but symmetric coupling coefficients, the* $\mathbb{C}^*$*-root count of the algebraic Kuramoto system coincides with the adjacency polytope bound, and as a corollary we showed that the algebraic Kuramoto system is Bernshtein-general.* The proof is constructive, and it produces a homotopy continuation method for computing all zeros. For Question 1.2, we provided a graph-theoretic description of the *exceptional coupling coefficients for which the* $\mathbb{C}^*$*-root count drops below the generic root count.* For Question 1.3, we established sufficient conditions on many families of networks where *there will be non-isolated real and complex zero sets* for these systems through explicit constructions.

While the analysis for the last two questions required some topological restrictions, it appears hopeful that the approach taken here can be generalized to other networks. We hope our work will spark interest in the full analysis of the typical and atypical solutions to Kuramoto equations.

Finally, we speculate that the explicit connection between the root count of the algebraic Kuramoto equations and the normalized volume of adjacency polytopes may also allow algebraic geometers to directly contribute to the geometric study of adjacency polytopes.

Acknowledgments. This project is inspired by a series of discussion the first named author had with Anton Leykin, Josephine Yu, and Yue Ren between 2017 and 2018. The first named author learned much about the structure of adjacency polytopes (symmetric edge polytopes) from Robert Davis, Alessio D'Alì, Emanuele Delucchi, and Mateusz Michałek. The authors thank Paul Breiding, Paul Helminck, and Davide Sclosa for their comments on an earlier version of this manuscript.

Appendix A. Notation. Here, we list notation used in this paper that may not be standard.

$\mathbb{C}\{\tau\}$ The field of Puiseux series in τ with complex coefficients is denoted $\mathbb{C}\{\tau\}$. Only convergent series representing germs of one-dimensional analytic varieties will be relevant.

$\mathcal{C}(P, \Delta_\omega)$ The closed secondary cone of a regular subdivision Δ_ω of a polytope P.

$\Sigma_\omega(P)$ The regular subdivision of a point configuration P induced by a lifting function $\omega : P \to \mathbb{Q}$.

$\check{\nabla}_G$ The point configuration associated with the adjacency polytope derived from a connected graph G. It is defined to be $\{\pm(\vec{e}_i - \vec{e}_j) \mid \{i,j\} \in \mathcal{E}(G)\} \cup \{\vec{0}\}$.

$\check{\nabla}_G^\omega$ The "lifted" version of the point configuration $\check{\nabla}_G$ induced by a lifting function $\omega : \check{\nabla}_G \to \mathbb{Q}$. It consists of the points $(\vec{p}, \omega(\vec{p})) \subset \mathbb{R}^{n+1}$ for all $\vec{p} \in \check{\nabla}_G$.

$\vec{f}_{(G,K,\vec{w})}, \vec{f}_{(G,K)}, \vec{f}_G$ The algebraic Kuramoto system derived from a Kuramoto network $(G, K, \vec{w})$. If the choice of the natural frequencies $\vec{w}$ is not relevant (or assumed to be generic), the notation $\vec{f}_{(G,K)}$ is used. Similarly, if only graph topology is of relevance, we use $\vec{f}_G$.

$\vec{f}_G^*$ The randomized algebraic Kuramoto system, i.e., $R \cdot \vec{f}_G$ for a generic square matrix R.

$(G, K, \vec{w}), (G, K)$ A Kuramoto network. G is the underlying graph, $K = \{k_{ij} \mid \{i, j\} \in \mathcal{E}(G)\}$ with $k_{ij} = k_{ji}$ encodes the coupling coefficients, and $\vec{w} = (w_0, \ldots, w_n)^\top$ contains the natural frequencies.

$\mathrm{init}_{\boldsymbol{v}}(f)$ For a Laurent polynomial f in $x_1, \ldots, x_n$, the *initial form* of f with respect to a vector $\boldsymbol{v}$ is the Laurent polynomial $\mathrm{init}_{\boldsymbol{v}}(f)(\boldsymbol{x}) := \sum_{\vec{a} \in (S)_{\vec{v}}} c_{\vec{a}} \boldsymbol{x}^{\vec{a}}$, where $(S)_{\vec{v}}$ is the subset of S on which $\langle \boldsymbol{v} , \cdot \rangle$ is minimized. It is denoted $\mathrm{init}_{\boldsymbol{v}}(f)$. For a system $\vec{f} = (f_1, \ldots, f_q)$ of Laurent polynomials, $\mathrm{init}_{\boldsymbol{v}}(\vec{f}) = (\mathrm{init}_{\boldsymbol{v}}(f_1), \ldots, \mathrm{init}_{\boldsymbol{v}}(f_q))$.

$Q(\vec{H}), \check{Q}(\vec{H})$ For a digraph $\vec{H}$, its *incidence matrix* $Q(\vec{H})$ is the matrix with columns $\vec{e}_i - \vec{e}_j$ such that $(i, j) \in \mathcal{E}(\vec{H})$. Since we set $\vec{e}_0$ to be the zero vector, the first row is all zeros. Therefore, we instead consider the *reduced incidence matrix*, $\check{Q}(\vec{H})$, with $n = |\mathcal{V}(\vec{H})| - 1$ rows, which is the incidence matrix of $\vec{H}$ with the first row deleted. The ordering of the columns in both is arbitrary, but, when either matrix appears in the same context with other incidence vectors, a consistent ordering is assumed. Here, the adjective "reduced" emphasizes the fact that the labels for the nodes in the graph are $0, 1, \ldots$, and therefore, for a digraph $\vec{H}$ of $n + 1$ nodes, $\check{Q}(\vec{H})$ only has n rows.

$\mathrm{MV}(P_1, \ldots, P_n)$ Given n convex polytopes $P_1, \ldots, P_n \subset \mathbb{R}^n$, the *mixed volume* of $P_1, \ldots P_n$ is the coefficient of the monomial $\lambda_1 \cdots \lambda_n$ in the homogeneous polynomial $\mathrm{vol}_n(\lambda_1 P_1 + \ldots + \lambda_n P_n)$ where $P + Q = \{p + q \;:\; p \in P,\ q \in Q\}$ denotes the Minkowski sum and vol_n is the standard $n-$dimensional Euclidean volume.

$\mathcal{N}_G(i), \mathcal{N}^+_{\vec{G}}(i), \mathcal{N}^-_{\vec{G}}(i)$ For a graph G and a node i of G, $\mathcal{N}_G(i)$ is the set of nodes that are adjacent to i. Similarly, the other two are the adjacent nodes through outgoing and incoming arcs in a digraph, respectively.

Vol The normalized volume of a set in $\mathbb{R}^n$, which is defined to be $n!$ times the Euclidean volume. The usage is restricted to convex polytopes here, and we adopt the convention that $\mathrm{Vol}(X) = 0$, if X is not full dimensional.

Appendix B. Elementary lemmata.

We restate Lemma 3.3 and provide an elementary proof.

Lemma B.1. *For a generic symmetric lifting function ω for $\check{\nabla}_G$, let Δ be a simplex in Δ_ω. Then the digraph $\vec{G}_\Delta$ is acyclic, and its underlying graph G_Δ is a spanning tree of G.*

Proof. Let $(\vec{\alpha}, 1)$ be the upward pointing inner normal that defines the cell Δ as a projection of a lower facet of $\check{\nabla}^w_G$. Suppose $\vec{G}_\Delta$ has a simple directed cycle $i_1 \to \cdots \to i_m \to i_1$. Then

$$\left\langle \vec{\alpha} , \vec{e}_{i_k} - \vec{e}_{i_{k+1}} \right\rangle + 1 + \delta_{i_k, i_{k+1}} = 0 \quad \text{for } k = 1, \ldots, m,$$

where $i_{m+1} = i_1$. Summing these m equations produces $m + \sum_{k=1}^m \delta_{i_k, i_{k+1}} = 0$, which is not possible under the assumption that δ_{ij} are sufficiently close to 0. So $\vec{G}_\Delta$ must be acyclic.

Moreover, $\dim(\Delta) = n$, by assumption. That is, $\{\vec{e}_i - \vec{e}_j \mid (i, j) \in \vec{G}_\Delta\}$ is must span $\mathbb{R}^n$ as a set of vectors (since $\vec{0} \in \Delta$, by construction). Therefore, for every $i \in \{0, \ldots, n\}$, either $\vec{e}_i - \vec{e}_j \in \Delta$ or $\vec{e}_j - \vec{e}_i \in \Delta$ for some $j \in \{0, \ldots, n\} \setminus \{i\}$. That is, G_Δ must be spanning. ■

Now we restate Lemma 4.5 and provide a short proof.

Lemma B.2. *For a proper face $F \neq \varnothing$ of $\check{\nabla}_G$ whose facial subdigraph $\vec{G}_F$ consists of weakly connected components $\vec{H}_1, \ldots, \vec{H}_\ell$, there exist faces $F_1, \ldots, F_\ell \neq \varnothing$ of F such that $\vec{H}_i = \vec{G}_{F_i}$ and*

$$\operatorname{init}_F(\vec{f}_G^*)(\boldsymbol{x}) = \vec{0} \iff \operatorname{init}_{F_i}(\vec{f}_G^*)(\boldsymbol{x}) = \vec{0} \quad \textit{for each } i = 1, \ldots, \ell.$$

Proof. Let $V_i = \mathcal{V}(\vec{H}_i)$ for $i = 1, \ldots, \ell$ with $0 \in V_1$. We arrange the coordinates of $\mathbb{Z}^n$ according to the grouping $V_1, \ldots, V_\ell$ so that an inner normal vector $\boldsymbol{\alpha} \in \mathbb{R}^n$ that defines the face F of $\check{\nabla}_G$ is written as $\boldsymbol{\alpha} = \begin{bmatrix} \boldsymbol{\alpha}_1 & \cdots & \boldsymbol{\alpha}_\ell \end{bmatrix}$ where $\boldsymbol{\alpha}_i \in \mathbb{R}^{|V_i|}$ corresponds to nodes in V_i. Then for $i = 1, \ldots, \ell$,

$$\boldsymbol{v}_i := \begin{bmatrix} \mathbf{0}_{|V_1|+\cdots+|V_{i-1}|} & \boldsymbol{\alpha}_i & \mathbf{0}_{|V_{i+1}|+\cdots+|V_\ell|} \end{bmatrix} \in \mathbb{R}^n$$

defines a face F_i of $\check{\nabla}_G$ such that $\vec{H}_i = \vec{G}_{F_i}$.

By grouping the rows and columns of $\check{Q}(\vec{G}_F)$ according to the nodes and arcs in $H_1, \ldots, H_\ell$, $\check{Q}(\vec{G}_F)$ has the block structure

$$\check{Q}(\vec{G}_F) = \begin{bmatrix} \check{Q}(\vec{H}_1) & & \\ & \ddots & \\ & & \check{Q}(\vec{H}_\ell) \end{bmatrix}.$$

Therefore, the cycle form of $\operatorname{init}_F(\vec{f}_G^*) = \vec{0}$, i.e., $\check{Q}(\vec{G}_F)\left(\boldsymbol{x}^{\check{Q}(\vec{G}_F)} \circ \boldsymbol{a}(\vec{G}_F)\right)^\top = \vec{0}$, is equivalent to

$$\check{Q}(\vec{H}_i)\left(\boldsymbol{x}_i^{\check{Q}(\vec{H}_i)} \circ \boldsymbol{a}(\vec{H}_i)\right)^\top = \vec{0} \quad \text{for each } i = 1, \ldots, \ell,$$

where $\boldsymbol{x}_i$ contain the coordinates corresponding to nodes in $\vec{H}_i$. This is equivalent to $\operatorname{init}_{F_i}(\vec{f}_G^*)(\boldsymbol{x}) = \vec{0}$ for each $i = 1, \ldots, \ell$, by Lemma 4.3. ■

Similarly, we restate Lemma 4.6 and provide a simple proof.

Lemma B.3. *For a proper face $F \neq \varnothing$ of $\check{\nabla}_G$, let $G' = G[G_F]$ and F' be the embedding of F in $\check{\nabla}_{G'}$. Then $\operatorname{init}_F(\vec{f}_G^*)$ has a $\mathbb{C}^*$-zero if and only $\operatorname{init}_{F'}(\vec{f}_{G'}^*)$ has a $\mathbb{C}^*$-zero.*

Proof. Order the vertices of $\vec{G}_F$ so that

$$\check{Q}(\vec{G}_F) = \begin{bmatrix} \check{Q}(\vec{G}_{F'}) \\ 0 \end{bmatrix},$$

Write $\boldsymbol{x} = [\boldsymbol{x'}\ \boldsymbol{y}]$ where $\boldsymbol{x'}$ is the vector of variables appearing in $\operatorname{init}_{F'}(\vec{f}_{G'}^*)$, and let $e_1, \ldots, e_d$ be the arcs in $\vec{G}_F$ that are not in $\vec{G}_{F'}$. Then by Lemma 4.3 we want to show that

$$\check{Q}(\vec{G}_F)\left(\boldsymbol{x}^{\check{Q}(\vec{G}_F)} \circ \boldsymbol{a}(\vec{G}_F)\right)^\top = \vec{0} \quad \Leftrightarrow \quad \check{Q}(\vec{G}_{F'})\left(\boldsymbol{x'}^{\check{Q}(\vec{G}_{F'})} \circ \boldsymbol{a}(\vec{G}_{F'})\right)^\top = \vec{0}.$$

Observe that

$$\begin{aligned} \check{Q}(\vec{G}_F)\left(\boldsymbol{x}^{\check{Q}(\vec{G}_F)} \circ \boldsymbol{a}(\vec{G}_F)\right)^\top &= \begin{bmatrix} \check{Q}(\vec{G}_{F'}) \\ 0 \end{bmatrix}\left([\boldsymbol{x'}\ \boldsymbol{y}]^{\check{Q}(\vec{G}_F)} \circ [\boldsymbol{a}(\vec{G}_{F'})\ a_{e_1}\ \ldots a_{e_d}]\right)^\top \\ &= \check{Q}(\vec{G}_{F'})\left(\boldsymbol{x'}^{\check{Q}(\vec{G}_{F'})} \circ \boldsymbol{a}(\vec{G}_{F'})\right)^\top, \end{aligned}$$

proving the statement. ■

We recall Corollary 4.10 and provide an elementary proof.

Corollary B.4. *Let F, $\vec{T}$, $\boldsymbol{x}_{\vec{T}}$, and $\boldsymbol{\tau}_1, \ldots, \boldsymbol{\tau}_d$ be as in Definition 4.7, and let $\boldsymbol{\eta}_i = [\boldsymbol{\tau}_i, -\boldsymbol{e}_i]$ and $\vec{\eta}_i = \boldsymbol{\eta}_i^\top$ for $i = 1, \ldots, d$. Then, for nonzero $\lambda_1, \ldots, \lambda_d$, the tree solution $\boldsymbol{x}_{\vec{T}}(\lambda_1, \ldots, \lambda_d)$ is a solution to the facial system $\operatorname{init}_F(\vec{f}_G^*)$ if and only if*

$$\left(\sum_{k=1}^d \lambda_k \boldsymbol{\eta}_k\right)^{\vec{\eta}_i} \cdot \boldsymbol{a}(\vec{H})^{-\vec{\eta}_i} = 1 \quad \textit{for each } i = 1, \ldots, d.$$

Proof. We will repeat some of the steps in the proof of Lemma 4.9 for reference.

Suppose we have $\lambda_1, \ldots, \lambda_d$ for which the equations above hold. Then

$$\left(\sum_{k=1}^{d} \lambda_k \boldsymbol{\tau}_k\right)^{\vec{\tau}_i} \cdot \boldsymbol{a}(\vec{T})^{-\vec{\tau}_i} \cdot \alpha_i = -\lambda_i \quad \text{for } i = 1, \ldots, d.$$

Let $\boldsymbol{x}$ be the corresponding tree solution, i.e.,

$$\boldsymbol{x} = \boldsymbol{x}_{\vec{T}}(\lambda_1, \ldots, \lambda_d) = \left[\left(\sum_{k=1}^{d} \lambda_k \boldsymbol{\tau}_k\right) \circ \boldsymbol{a}(\vec{T})^{-I}\right]^{\check{Q}(\vec{T})^{-1}}.$$

Then

$$\left(\boldsymbol{x}^{\check{Q}(\vec{H})} \circ \boldsymbol{a}(\vec{H})\right)^{\top} = \begin{bmatrix} \left(\boldsymbol{x}^{\check{Q}(\vec{T})} \circ \boldsymbol{a}(\vec{T})\right)^{\top} \\ \boldsymbol{x}^{\vec{v}_1} \cdot \alpha_1 \\ \vdots \\ \boldsymbol{x}^{\vec{v}_d} \cdot \alpha_d \end{bmatrix} = \begin{bmatrix} \left(\sum_{k=1}^{d} \lambda_k \boldsymbol{\tau}_k\right)^{\top} \\ \left(\sum_{k=1}^{d} \lambda_k \boldsymbol{\tau}_k\right)^{\boldsymbol{\tau}_1} \boldsymbol{a}(\vec{T})^{-\boldsymbol{\tau}_1} \alpha_1 \\ \vdots \\ \left(\sum_{k=1}^{d} \lambda_k \boldsymbol{\tau}_k\right)^{\boldsymbol{\tau}_d} \boldsymbol{a}(\vec{T})^{-\boldsymbol{\tau}_d} \alpha_d \end{bmatrix} = \begin{bmatrix} \left(\sum_{k=1}^{d} \lambda_k \boldsymbol{\tau}_k\right)^{\top} \\ -\lambda_1 \\ \vdots \\ -\lambda_d \end{bmatrix}$$

which is in the null space of $\check{Q}(\vec{H})$. Thus, $\check{Q}(\vec{H})(\boldsymbol{x}^{\check{Q}(\vec{H})} \circ \boldsymbol{a}(\vec{H}))^{\top} = \vec{0}$. That is, $\boldsymbol{x}$ is a $\mathbb{C}^*$-solution to the facial system $\operatorname{init}_F(\vec{f}^*_G)$.

Conversely, suppose $\boldsymbol{x}$ is a $\mathbb{C}^*$-zero of the facial system $\operatorname{init}_F(\vec{f}^*_G)$, then by Lemma 4.9, it is given by a tree solution. I.e., $\boldsymbol{x} = \boldsymbol{x}_{\vec{T}}(\lambda_1, \ldots, \lambda_d)$ for some $\lambda_1, \ldots, \lambda_d$. From the equation above,

$$\left(\boldsymbol{x}^{\check{Q}(\vec{H})} \circ \boldsymbol{a}(\vec{H})\right)^{\top} = \begin{bmatrix} \left(\sum_{k=1}^{d} \lambda_k \boldsymbol{\tau}_k\right)^{\top} \\ \left(\sum_{k=1}^{d} \lambda_k \boldsymbol{\tau}_k\right)^{\boldsymbol{\tau}_1} \boldsymbol{a}(\vec{T})^{-\boldsymbol{\tau}_1} \alpha_1 \\ \vdots \\ \left(\sum_{k=1}^{d} \lambda_k \boldsymbol{\tau}_k\right)^{\boldsymbol{\tau}_d} \boldsymbol{a}(\vec{T})^{-\boldsymbol{\tau}_d} \alpha_d \end{bmatrix}$$

must be in the null space of $\check{Q}(\vec{H})$. Since the vectors $(\boldsymbol{\tau}_1, -\boldsymbol{e}_1)^{\top}, \ldots, (\boldsymbol{\tau}_d, -\boldsymbol{e}_d)^{\top}$ form a basis for this null space. Therefore,

$$\left(\sum_{k=1}^{d} \lambda_k \boldsymbol{\tau}_k\right)^{\vec{\tau}_i} \cdot \boldsymbol{a}(\vec{T})^{-\vec{\tau}_i} \cdot \alpha_i = -\lambda_i \quad \text{for } i = 1, \ldots, d,$$

which is equivalent to the conclusion. ■

REFERENCES

[1] P. Ashwin, C. Bick, and O. Burylko, *Identical Phase Oscillator Networks: Bifurcations, Symmetry and Reversibility for Generalized Coupling*, Frontiers in Applied Mathematics and Statistics, 2 (2016), p. 7, https://doi.org/10.3389/fams.2016.00007, https://arxiv.org/abs/1603.07937.

[2] J. Baillieul and C. Byrnes, *Geometric critical point analysis of lossless power system models*, IEEE Transactions on Circuits and Systems, 29 (1982), pp. 724–737, https://doi.org/10.1109/tcs.1982.1085093.

[3] D. N. Bernshtein, *The number of roots of a system of equations*, Functional Analysis and Its Applications, 9 (1975), pp. 183–185, https://doi.org/10.1007/bf01075595.

[4] M. Breakspear, S. Heitmann, and A. Daffertshofer, *Generative models of cortical oscillations: Neurobiological implications of the Kuramoto model*, Frontiers in Human Neuroscience, 4 (2010), https://doi.org/10.3389/fnhum.2010.00190.

[5] P. Breiding, M. Michałek, L. Monin, and S. Telen, *The algebraic degree of coupled oscillators*, 2022, https://doi.org/10.48550/ARXIV.2208.08179, https://arxiv.org/abs/2208.08179.

[6] T. Chen, *On the equality of BKK bound and birationally invariant intersection index*, arXiv, (2018), https://arxiv.org/abs/1812.05408.

[7] T. Chen, *Directed acyclic decomposition of Kuramoto equations*, Chaos: An Interdisciplinary Journal of Nonlinear Science, 29 (2019), p. 093101, https://doi.org/10.1063/1.5097826, https://arxiv.org/abs/1903.04492.

[8] T. Chen, *Unmixing the Mixed Volume Computation*, Discrete & Computational Geometry, 62 (2019), pp. 55–86, https://doi.org/10.1007/s00454-019-00078-x.

[9] T. Chen and R. Davis, *A toric deformation method for solving Kuramoto equations on cycle networks*, Nonlinear Dynamics, (2022), pp. 1–20, https://doi.org/10.1007/s11071-022-07550-z.

[10] T. Chen, R. Davis, and E. Korchevskaia, *Facets and facet subgraphs of adjacency polytopes*, arXiv, (2021), https://arxiv.org/abs/2107.12315.

[11] T. Chen, R. Davis, and D. Mehta, *Counting Equilibria of the Kuramoto Model Using Birationally Invariant Intersection Index*, SIAM Journal on Applied Algebra and Geometry, 2 (2018), pp. 489–507, https://doi.org/10.1137/17m1145665.

[12] T. Chen and E. Korchevskaia, *Graph edge contraction and subdivisions for adjacency polytopes*, arXiv, (2019), https://arxiv.org/abs/1912.02841.

[13] T. Chen and D. Mehta, *On the Network Topology Dependent Solution Count of the Algebraic Load Flow Equations*, IEEE Transactions on Power Systems, 33 (2017), pp. 1451–1460, https://doi.org/10.1109/tpwrs.2017.2724030.

[14] O. Coss, J. D. Hauenstein, H. Hong, and D. K. Molzahn, *Locating and counting equilibria of the Kuramoto model with rank-one coupling*, SIAM J. Appl. Algebra Geom., 2 (2018), pp. 45–71, https://doi.org/10.1137/17M1128198, https://doi-org.ezproxy.library.wisc.edu/10.1137/17M1128198.

[15] A. D'Alì, E. Delucchi, and M. Michałek, *Many Faces of Symmetric Edge Polytopes*, The Electronic Journal of Combinatorics, 29 (2022), https://doi.org/10.37236/10387.

[16] F. Dörfler and F. Bullo, *Synchronization and transient stability in power networks and non-uniform kuramoto oscillators*, in Proceedings of the 2010 American Control Conference, 2010, pp. 930–937, https://doi.org/10.1109/ACC.2010.5530690.

[17] J. Grainger and W. Stevenson, *Power System Analysis*, McGraw-Hill international editions, McGraw-Hill Education, 1994, https://books.google.com/books?id=NBIoAQAAMAAJ.

[18] S. Guo and F. Salam, *Determining the solutions of the load flow of power systems: Theoretical results and computer implementation*, 29th IEEE Conference on Decision and Control, (1990), pp. 1561–1566 vol.3, https://doi.org/10.1109/cdc.1990.203876.

[19] Y. Guo, D. Zhang, Z. Li, Q. Wang, and D. Yu, *Overviews on the applications of the kuramoto model in modern power system analysis*, International Journal of Electrical Power & Energy Systems, 129 (2021), p. 106804, https://doi.org/https://doi.org/10.1016/j.ijepes.2021.106804, https://www.sciencedirect.com/science/article/pii/S0142061521000442.

[20] H. Harrington, H. Schenck, and M. Stillman, *Kuramoto oscillators: algebraic and topological aspects*, 2023, https://arxiv.org/abs/2312.16069.

[21] P. A. Helminck and Y. Ren, *Generic root counts and flatness in tropical geometry*, arXiv, (2022), https://arxiv.org/abs/2206.07838.

[22] A. Higashitani, K. Jochemko, and M. Michałek, *Arithmetic aspects of symmetric edge polytopes*, Mathematika, 65 (2019), pp. 763–784, https://doi.org/10.1112/s0025579319000147, https://arxiv.org/abs/1807.07678.

[23] B. Huber and B. Sturmfels, *A polyhedral method for solving sparse polynomial systems*, Mathematics of Computation, 64 (1995), pp. 1541–1555, https://doi.org/10.1090/s0025-5718-1995-1297471-4.

[24] Y. Kuramoto, *International Symposium on Mathematical Problems in Theoretical Physics, January 23–29, 1975, Kyoto University, Kyoto/Japan*, Lecture Notes in Physics, (2005), pp. 420–422, https://doi.org/10.1007/bfb0013365.

[25] A. G. Kushnirenko, *Newton polyhedron and Milnor numbers*, Functional Analysis and Its Applications, 9 (1975), pp. 71–72, https://doi.org/10.1007/bf01078188.

[26] T.-Y. Li, T. Sauer, and J. A. Yorke, *Numerical Solution of a Class of Deficient Polynomial Systems*, SIAM Journal on Numerical Analysis, 24 (1987), pp. 435–451, https://doi.org/10.1137/0724032.

[27] J. Lindberg, *Convex Algebraic Geometry with Applications to Power Systems, Statistics and Optimization*, PhD thesis, University of Wisconsin-Madison, 2022, https://www.proquest.com/dissertations-theses/convex-algebraic-geometry-with-applications-power/docview/2669513664/se-2.

[28] J. Lindberg, N. Boston, and B. C. Lesieutre, *Exploiting symmetry in the power flow equations using monodromy*, ACM Commun. Comput. Algebra, 54 (2020), pp. 100–104.

[29] J. Lindberg, A. Zachariah, N. Boston, and B. Lesieutre, *The Distribution of the Number of Real Solutions to the Power Flow Equations*, IEEE Transactions on Power Systems, PP (2022), pp. 1–1, https://doi.org/10.1109/tpwrs.2022.3170232.

[30] T. Matsui, A. Higashitani, Y. Nagazawa, H. Ohsugi, and T. Hibi, *Roots of Ehrhart polynomials aris-*

ing from graphs, Journal of Algebraic Combinatorics, 34 (2011), pp. 721–749, https://doi.org/10.1007/s10801-011-0290-8.

[31] D. K. Molzahn, D. Mehta, and M. Niemerg, *Toward Topologically Based Upper Bounds on the Number of Power Flow Solutions*, 2016 American Control Conference (ACC), (2016), pp. 5927–5932, https://doi.org/10.1109/acc.2016.7526599, https://arxiv.org/abs/1509.09227.

[32] A. P. Morgan and A. J. Sommese, *Coefficient-parameter polynomial continuation*, Applied Mathematics and Computation, 29 (1989), pp. 123–160, https://doi.org/10.1016/0096-3003(89)90099-4.

[33] A. Postnikov, *Permutohedra, Associahedra, and Beyond*, International Mathematics Research Notices, 2009 (2009), pp. 1026–1106, https://doi.org/10.1093/imrn/rnn153.

[34] F. A. Rodrigues, T. K. D. Peron, P. Ji, and J. Kurths, *The kuramoto model in complex networks*, Physics Reports, 610 (2016), pp. 1–98, https://doi.org/https://doi.org/10.1016/j.physrep.2015.10.008, https://www.sciencedirect.com/science/article/pii/S0370157315004408. The Kuramoto model in complex networks.

[35] D. Sclosa, *Kuramoto networks with infinitely many stable equilibria*, 2022, https://doi.org/10.48550/ARXIV.2207.08182, https://arxiv.org/abs/2207.08182.

[36] M. K. S. Yeung and S. H. Strogatz, *Time delay in the kuramoto model of coupled oscillators*, Phys. Rev. Lett., 82 (1999), pp. 648–651, https://doi.org/10.1103/PhysRevLett.82.648, https://link.aps.org/doi/10.1103/PhysRevLett.82.648.